

INTEGRATION OF HYPERSPECTRAL IMAGING SYSTEM FOR
OPTIMIZED DATA ACQUISITION AND CONTROL
TO REVOLUTIONIZE PATHOLOGY
APPLICATIONS

by

DIPEN RANA

Presented to the Faculty of the Graduate School of
The University of Texas at Arlington in Partial Fulfillment
of the Requirements
for the Degree of

MASTER OF SCIENCE IN BIOMEDICAL ENGINEERING

THE UNIVERSITY OF TEXAS AT ARLINGTON

DECEMBER 2008

Copyright © by DIPEN RANA 2008

All Rights Reserved

I dedicate this thesis to my Dad and Mom who have worked very hard and made so many sacrifices to help me pursue my dreams.

ACKNOWLEDGEMENTS

I wish to take this opportunity to express my gratitude to all individuals who have helped me during this thesis work. I would like to thank my supervising professor Dr. Harold 'Skip' Garner, for being an extremely inspiring and encouraging mentor and providing me with invaluable advice in the course of my graduate degree. Special thanks to Dr. Michael Huebschman for his suggestions and insights into this project and for being a great friend. I am extremely grateful to Dr. Hanli Liu and Dr. George Alexandrakis for their interest in my research work and for accepting the invitation to be my committee members. I also express my sincere gratitude to Dr. Jonathan Uhr, who taught me the basics of cancer immunology, to Linda and Kay for all the administrative help and friendly encouragement they have showered me with, and to all the members of the Garner lab. I also wish to thank my friend Jyoti who has proofread my thesis and helped in every possible way in order for me to complete this thesis. And most importantly, I am indebted to my family my parents Dad and Mom, and my Nayan uncle who have always been there for me. I would not have made it this far without their help, encouragement and support throughout my life.

Thank you Dad, for being my role model and my greatest pillar of support.

November 24, 2008

ABSTRACT

INTEGRATION OF HYPERSPECTRAL IMAGING SYSTEM FOR OPTIMIZED DATA ACQUISITION AND CONTROL TO REVOLUTIONIZE PATHOLOGY APPLICATIONS

Dipen Rana, M S

The University of Texas at Arlington, 2008

Supervising Professor: Harold "Skip" Garner

Detecting and measuring the interactions and expression levels of tumor markers in a cancerous cell are quintessential in the prognosis and management of cancer. These have propagated the need to develop better microscopic imaging techniques to understand the cellular structure and its functional behavior. Pathologist use techniques such immunohistochemistry and in situ hybridization to measure and detect these tumor marker expression levels. Fluorophores are used in these techniques as fluorescent tags to identify the tumor markers. These fluorophores have unique absorption and emission spectrum, making them useful to not only identify but also quantify the concentration levels of the markers. This allows us to tag multiple fluorophores within a single cell. Although useful it is limited by the ability to resolve the overlapping emission spectra of the multiplexed fluorophores. This limits the total number of fluorophores that can be used to identify the different components within a single cell. Hyperspectral imaging used in astronomy for remote sensing of earth collects

contiguous band of wavelengths over each pixel in image. This ability to provide spectral signatures associated with spatial resolution can be used to deconvolve the overlapping spectra of multiplexed fluorophores. This can be achieved by matching the standard emission spectrum of each multiplexed fluorophore with spectra at each pixel in the image. This enables to not only deconvolve the fluorophores but also quantify the contribution of each fluorophore at any pixel in an image.

At the center of hyperspectral imaging system is a microscope coupled with an imaging spectrograph to disperse the incoming light into its components, a CCD camera focused at the exit port of the spectrograph is used to record the information and a stage motor positioned onto the microscope helps to move the sample across the optical path to cover the entire region of interest. This propels the need to precisely control the major components of hyperspectral imaging system through automated data acquisition software to provide high resolution data. This software also needs to provide a dynamic user interface along with complete automated control over all these components to emulate actions of a trained microscope operator thus making it commercially viable and ready for transition into a pathology lab.

This thesis work describes the integration of such a hyperspectral imaging system to provide a complete automated control and data acquisition software named Xanoscope®. It validates the features and functionality of Xanoscope® by comparing it against the specifications from individual hardware components. It further demonstrates that the Xanoscope® can repetitively used to identify and quantify the expression levels of up to 10 fluorophores conjugated to tumor markers of breast cancer cell lines as well as samples from breast cancer patients along with normal cells. Xanoscope® thus aids to revolutionize the diagnoses and monitoring of cancer and its response to therapeutic regimes.

TABLE OF CONTENTS

ACKNOWLEDGEMENTS.....	iv
ABSTRACT	v
LIST OF ILLUSTRATIONS	viii
LIST OF TABLES	xii
Chapter	
1. INTRODUCTION	1
1.1 Hyperspectral Imaging.....	4
1.2 Fluorophores and its Application in Hyperspectral Imaging	7
1.3 Pseudocoloring.....	8
1.4 Research problem	10
2. METHODS.....	11
2.1 Hyperspectral Imaging Microscopy System	11
2.1.1 Epi-Fluorescence Microscope System	13
2.1.2 Imaging Spectrograph	17
2.1.3 Stage Motor	20
2.1.4 Charge Couple Device (CCD) Camera	21
2.1.4.1 Binning.....	27
2.2 Software.....	32
2.2.1 Characterizing the Hardware.....	35
2.2.1.1 Camera.....	36

2.2.1.2 Spectrograph	39
2.2.1.3 Stage Motor	40
2.2.2 Experimental Protocol	43
2.2.3 Data Acquisition using Xanoscope®	44
3. RESULTS AND DISCUSSION	53
3.1 Software Validation.....	53
3.1.1 Determination of Spatial Resolution	53
3.1.2 Determination of the Field of View	54
3.1.3 Validating the Linearity of CCD Camera through Xanoscope....	55
3.1.4 Validating Gain Settings of the Camera	56
3.1.5 Validation of Accumulations Functionality of Xanoscope.....	57
3.1.6 Validating Xanoscope's Accurate and Precise Control over the Movement of Stage	60
3.2 Performance Evaluation	61
3.2.1 Characterization of Multiplexed Fluorophores.....	61
3.2.2 Statistical analysis of quantitative data extracted from Multiplexed Fluorophores using Xanoscope	66
4. CONCLUSION AND FUTURE GOALS.....	68
REFERENCES	69
BIOGRAPHICAL INFORMATION	72

LIST OF ILLUSTRATIONS

Figure		Page
1.1	Sample Hyperspectral Imaging System	5
1.2	(a) Hyperspectral Data Cube and (b) Composite Image	6
1.3	Stokes Shift	8
1.4	H&E Stained Tissue Sample and an Unstained tissue sample.....	9
2.1	Hyperspectral Imaging Microscopy System	12
2.2	Schematic Cut Way Of Olympus Ix Epi-Fluorescence Inverted Microscope	13
2.3	Spectrum of Polychromatic White Light in Visible Range.	14
2.4	Emission Spectrum of Mercury and a Xenon Arc Lamp in the Visible Range ..	14
2.5	Standard Filter Cube	15
2.6	Optical path of Illumination Source through the Microscope.....	16
2.7	Typical Dispersion Grating in Imaging Spectrograph.....	17
2.8	Similar looking Spectra Pro 500i Spectrograph.....	18
2.9	Schematic Working of imaging spectrograph.....	18
2.10	Relative Intensity Response to Spectrometer Entrance Slit Width	19
2.11	Schematic Working of X-Y Stage Motor	20
2.12	A Typical Joy Stick for manual control of the micro-mover LEP stage.....	21
2.13	A Typical Quantix 1602E air cooled CCD Camera	22
2.14	Analogy for Charge transfer in a Typical CCD Camera	24
2.15	Quantum Efficiency for Quantix 1602E CCD Camera	26
2.16	Schematic of a Typical Charge Transfer in a CCD Array.....	28
2.17	A Typical Frame Readout for 1X1 Binning process	29

2.18	Schematic of charge transfer for 1X1 binning in a CCD Camera	29
2.19	A Typical Frame Readout for 2X2 Binning process	30
2.20	Schematic of Charge transfer for 2X2 binning in a CCD Camera.....	31
2.21	Typical Pixel Binning	31
2.22	Xanoscope® application Software Splash Screen.....	32
2.23	Flow Chart of Xanoscope®	33
2.24	Schematic of Construction of a typical Hyperspectral Data Cube	34
2.25	Main Window of Xanoscope® Software.....	35
2.26	Camera Settings dialog Box of Xanoscope® to control various device parameters of Quantix 1602E CCD camera	36
2.27	Different Exposure Modes.....	37
2.28	SpectraPro ver3.35.....	39
2.29	Typical Character Frame for RS232 Communication	40
2.30	Typical Stage Settings Dialog Box in Xanoscope®.....	42
2.31	A Detailed Flowchart of Xanoscope's Data Acquisition Process in HMI System.....	45
2.32	A Typical Scan Settings Dialog Box in Xanoscope® to Input Relevant Information for Scan Procedure.....	46
2.33	A Sample slide with cells focused at the center of field of view of microscope	49
2.34	A Typical Resultant X-Y Composite Grayscale Image.....	50
2.35	A Typical Scan Information Window Displayed along Resultant X-Y Composite Image A: Scan Information, B: Parameters Information, C: Analysis Information including Spatial Dimensions and Intensity counts from the composite image.....	51
2.36	Quick Review of Spectrum in Hyperspectral Data Cube using (a) Point Spectrum and (b) Row Spectrum.....	52
3.1	Figure shows spatial resolution of a pixel for a 2x2 binned image image at 60X objective and 72µm slit width and 768x512 pixels.....	54
3.2	Figure shows the validation of CCD linearity using data acquired by Xanoscope.....	55
3.3	Figure shows the average intensity counts (gray levels) in each image at 3 different gain settings.....	56

3.4	Validating linear increase in average counts in composite image with linear increase in number of accumulations i.e. 1,3,5,7 and 9.	58
3.5	Figure shows composite images acquired 1,3,5,7 and 9 accumulations.	59
3.6	Figure shows the precise control of Xanoscope over micro-mover stage.	60
3.7	Figure shows standard emission spectra of 12 fluorophores.	62
3.8	(a) Reference spectra for two sample fluorophore R1 and R2 and (b) Spectra at any pixel in an image.	63
3.9	Figure shows process of evaluating the contribution each fluorophore algorithmically.	64
3.10	Figure shows visualization individual contribution of fluorophores-antibody conjugates in MCF7- breast cancer cell, Daudi - Human Burkitt's lymphoma cell line and Touch preps from breast cancer patients and also normal breast cells.	65
3.11	Figure shows graph of statistical analysis of the quantitative data acquired using Xanoscope.	67

LIST OF TABLES

Table		Page
2.1	Filter Cube Specifications ©Olympus microscopy center	15
2.2	Typical Quantix 1602E CCD Camera Specification Sheet.....	23
2.3	Quantix 1602E CCD Camera Gain Specifications ©Photometrics	25
2.4	RS232 Interface Settings for Stage Motor.....	41
2.5	Absorption and Emission Wavelengths of Each of the 10 fluors along with its conjugated antibody and false color used to display each fluor	44
3.1	Figure shows Marker table of the ten fluorophores-antibody conjugated with peak absorption and emission wavelengths of each fluorophores along with localization of its expression in the cell.....	62
3.2	Table shows the expression of fluorophore-antibody conjugate for MCF7 and Daudi cell line and also from cells of cancer patient and normal breast cells.....	66

CHAPTER 1

INTRODUCTION

Over the years the quest to identify and characterize cellular interactions and pathways to improve classification and prognosis of diseases, such as cancer, has led to development of various microscopy techniques. Multicolor Fluorescent In-Situ Hybridization (M-FISH) is one such technique that enables selective labeling of various DNA sequences and proteins with fluorescently labeled probes to detect expression levels of target molecules within the cell [1]. These complex labeled probes imaged using fluorescence microscopy imaging provide visualization and the contribution of the individual fluorescent probes within a single cell. Levels of estrogen, progesterone and Her-2 receptor, commonly used in breast cancer diagnosis, can be detected and measured using this technique [2]. These labeled probes are then visually examined and classified subjectively by a pathologist. This limits its use to only 2 or 3 multiplexed fluorescent probes due to the inability to visually resolve two spectrally overlapping fluorescent probes of different colors within same cellular component. Another technique, Immunohistochemistry (IHC), uses fluorescent dyes to visualize localization of antigens and proteins by binding fluorescent dyes to antibodies which in turn bind to antigens and proteins. Despite numerous fluorescent color markers, typically, only a single color is used per slide. If more than one antigen needs to be analyzed, then serial sections with a different antibody is applied to each. This limits the use of IHC if the co-expression of antigens in single cell needs to be investigated [3]. It also means that the data from each marker on each thin slice must be associated with each other slice. This makes it a labor intensive, error prone and imprecise operation.

The cellular organization and biochemical composition of a tissue interact with light distinctly; this gives rise to its spectral variations. This phenomenon can be utilized in pathology to extract information about the structural and functional status of the tissue [6]. This basic difference among cellular structures can be exploited using multispectral imaging techniques. Multispectral imaging techniques use precise measurements of optical spectra at every pixel of an image. It uses the principle of spectroscopy, how different materials uniquely absorb and emit light at different wavelengths based on their molecular composition. This enables us to obtain an image where each pixel contains the complete spectral signature of a material across its range of wavelengths. This helps us to resolve issues related to the multiplexing of fluorescent dyes and unmixing of spectrally overlapping fluorophores within a single image [2-4]. Multispectral imaging systems consist of a microscope, filters for spectral selection and a charge coupled device (CCD) camera to record the data [5]. A multispectral imager thus produces individual discrete images with relatively wide spectral bands. Although effective, this technique requires individual single band pass excitation/emission filter sets for each fluorophores used in multiplexing. This limits its use to the total number of filter sets that can be used for multiplexing. Multispectral imaging is also limited to measuring intensity within only a selected wavelength band. Although this allows characterization of multiplexed fluorophores, it limits the spectra of data that can be defined by the characteristics of its optical filters used [5]. Another spectral imaging technique employs a Sagnac interferometer which splits the emission spectrum from a microscope into two beams. It then allows these two beams to interfere and the pattern developed is focused onto a CCD detector system [4]. This data acquired is then analyzed using Fast Fourier Transform (FFT) algorithm to deconvolve spectral signatures [2] at each image pixel. Although useful, interferometric instruments are known to have limitations with the image registration and lateral coherence due to the beam splitter design [2]. Such limitations of multispectral imaging and interferometric instruments have lead to use of a better system that is capable of collecting broad contiguous bands of wavelengths over the region of interest. Hyperspectral imaging system has been long used for satellite imaging and remote

sensing by NASA as in Hyperion instrument to classify, and quantify materials present in our own planet's land mass [5]. The primary goal in remote sensing applications is to identify the contribution of individual constituents such as water, soil, vegetation in each pixel in the area of interest. The main purpose of using hyperspectral imaging over multispectral imaging is its uniqueness to produce images over the contiguous spectral band in a single pass. This offers exhaustive spectroscopic analysis over the region of interest. Using hyperspectral imaging, we obtain a 3 dimensional image i.e. an X Y spatial image at an arbitrarily large number of wavelengths [2-7]. Collecting a stack of such images over an area of interest, a data cube [Figure1.2] can be developed with each pixel representing its X Y spatial dimensions and an entire contiguous band of wavelengths. Furthermore using spectral unmixing algorithms, the proportion of each constituent (fluorophores) present in each pixel of the composite image can be measured .This can be easily achieved by comparing standard spectral signature of individual constituents (fluorophores) with spectrum of each pixel in composite.

Hyperspectral imaging techniques can be applied to the field of pathology to investigate the characteristic and functional behavior of cellular components in various environmental conditions i.e. normal or diseased conditions. A prototype hyperspectral imaging system [2], developed previously by Dr. Garner and Roger Schultz, records a single line of visible emission spectrum from the specimen slide using a microscope, a spectrograph and a CCD camera. Multiple such exposures are recorded by the CCD as it steps across the slide to cover the region of interest. On each step, one dimension is space and the other is wavelength. The software then controls the entire acquisition process and correlates its spatial and spectral information. This reduces the long acquisition time required for the process and also eliminates the need for multiple optical bandpass filters. Fluorophores are widely used in pathology to visualize the various cellular components and organelles. It is based on the principle of fluorescence which employs molecules that absorb energy at specific wavelengths and then promptly re-emits energy at different wavelengths [2]. This property can be exploited using hyperspectral imaging and fluorescence labeling techniques. Just like the FISH method

discussed previously, multiplexed fluorophores conjugated to the cellular structures of a tissue sample can be used to investigate multiple target molecules within a cell. By decomposing this hyperspectral data cube developed and using the individual fluorophore's standard emission spectral signatures; contributions of the individual fluorophores in cellular structures within the cell can be measured.

This thesis describes the development of a highly automated and robust system to integrate these techniques to provide exhaustive spatial and spectral information for detailed analysis and classification.

1.1 Hyperspectral Imaging

The Hyperspectral imaging system collects light waves at a multitude of wavelengths for each pixel in an image [2]. Collecting a stack of such wavelength images by stepping across the region of interest and adding them together creates a "hyperspectral data cube" [2]. It correlates the spatial dimension with the spectral dimension for every pixel on the image. The spectrum of a material is a property of how it responds to light at different wavelengths. Now in order to investigate multiple cellular structures and protein expression that control signaling pathways in cells, the pathologist use fluorescent dyes to label them. These individual fluorescent dyes respond distinctly to light at different wavelengths. If multiple fluorescent dyes are used within a single cell, its overlapping spectra in each pixel poses a limitation to the use of dyes since the spectrum obtained cannot be distinguished by eye. We can overcome this limitation with the use of hyperspectral imaging as we record spectral signatures at each pixel in an image. Given an appropriate set of the fluorescent dye standards, the algorithms can quantify the absolute amount of a dye in each pixel. An overview of the hyperspectral imaging system is shown in Figure 1.1. It consists of a standard epi-fluorescence inverted microscope and set of standard filter cubes for traditional eyepiece visualization of fluorescent dyes.

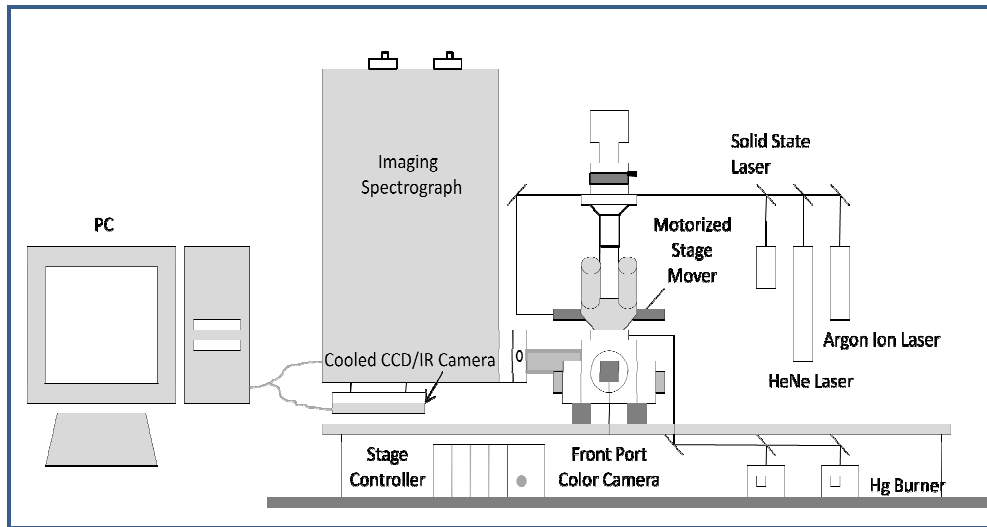


Figure 1.1 Sample Hyperspectral Imaging System

Multiple excitation light sources and band pass filters can be used to select an appropriate bandwidth of excitation wavelengths to visualize various fluorescent dyes. Illumination from the microscope sample is then passed through the microscope side port onto a narrow slit of the spectrograph. This slit entrance is optically coupled to the exit port of the spectrograph. Only a single line of the image corresponding to the slit width is allowed into the spectrograph at a time. This single line corresponding to the white light is separated into its entire spectrum of contiguous wavelengths by the spectrograph using diffraction grating principle. Multiple such single lines from the sample are scanned and recorded onto a CCD camera by stepping across the microscope slide using a programmable stage motor. A composite image can be created by adding these slices together which correspond to a hyperspectral data cube as shown in Figure 1.2 [2].

Xanoscope, a "VC++" based application software, has been developed to control this entire process and to store individual raw images on to a PC. It also builds and displays a composite image by adding these individual slices together and stores it along with raw images for further analysis. Emission spectrum at any pixel of the image can also be visualized by using a mouse-over function. This software also displays various parameters with which the system was initialized and stores them for further analysis. The spectrum at each pixel of the composite

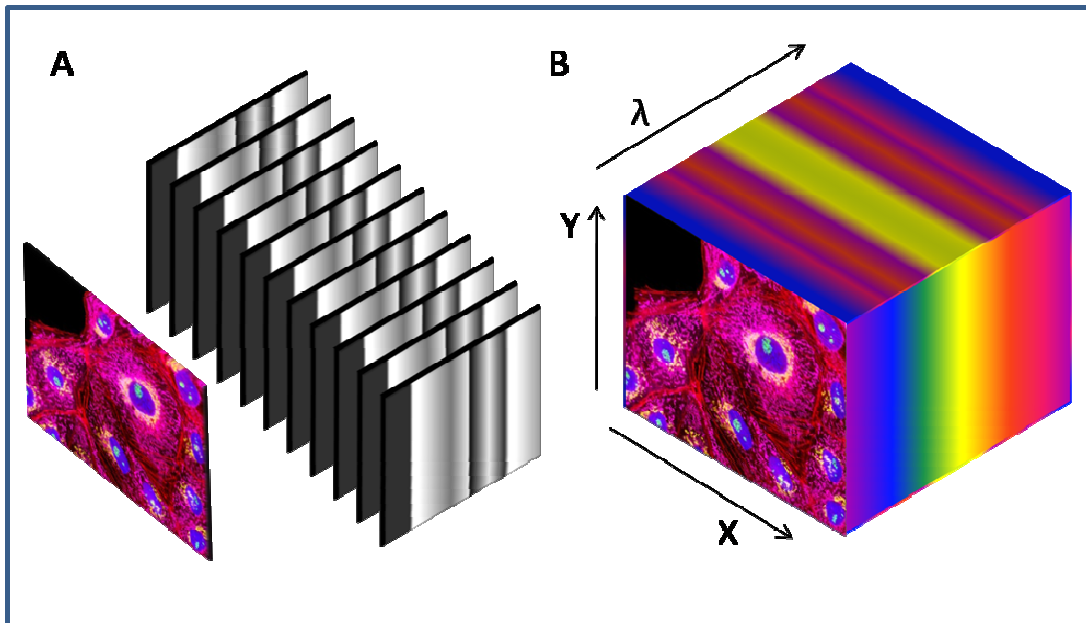


Figure 1.2 (a) Hyperspectral Data Cube and (b) Composite Image

image enables us to study the characteristic behavior and functions of the cellular structures and quantify the expression levels of each dye in any pixel of image. Thus, this quantification capability can be used to investigate expression of proteins and organelle receptors within a cell by labeling them with fluorescent dyes. The Hyperspectral imaging microscopy system produces real time images and allows its quick analysis, prompting very precise quantitative measurement of multiple biomarkers on a variety of pathology sample types. This revolutionizes pathology applications for monitoring diseases like cancer, and its response to therapeutic drugs [2].

1.2 Fluorophores and its application in hyperspectral imaging

Fluorescence based imaging is widely used in pathology to identify the structural components and dynamic process within the cells and tissue samples. Fluorophores are chemical compounds that are conjugated to antibodies to allow us to monitor the interactions and quantify the expression of multiple cellular structures and molecules in a single cell [Olympus Inc.]. This fluorophores are characterized according to their absorption and emission spectrum. Photons absorbed by the fluorophores bring them to an excited state. This excited fluorophore then relaxes to lower state by emitting energy in form of photons. Energy is lost in transition from excited state to ground state as per Stokes shift phenomenon. Thus emission peak of a fluorophore is of longer wavelength than its excitation peak wavelength, which corresponds to principle of fluorescence as shown in Figure1.3. In order to achieve high fluorescence emission intensity, fluorophore should be excited near or at the maximum of the excitation curve. The efficiency with which a particular fluorophore absorbs a photon of the excitation light is a function of the molecular cross-section [Nikon microscopy]. This proves to be an extremely powerful way of providing contrast based microscopic imaging. For example fluorophore such as DAPI binds selectively to DNA and thus is regularly used as a counter stain for the nucleus of a cell [invitrogen]. Multiple fluorophores can also be simultaneously hybridized to various cellular structures and molecules within a single cell. Such multiplexing enables one to investigate the cellular interactions and quantify expression levels of cellular structures within a single cell. The main obstacle in using multiplexed fluorophores lies in its ability to deconvolve overlapping spectra of fluorophores within a single cell. Hyperspectral imaging proves extremely beneficial in this regard due to its inherent property to acquire an image with its contiguous bands of spectral signatures allied to it. Thus a tissue sample with multiplexed fluorophores can be scanned using hyperspectral imaging microscopy to generate slices of an image. The composite image thus created contains the contiguous bands of spectral signatures allied to its spatial dimension. Using spectral unmixing algorithms we can easily identify the contribution of each fluorophore at any pixel in the composite image. This can be achieved by

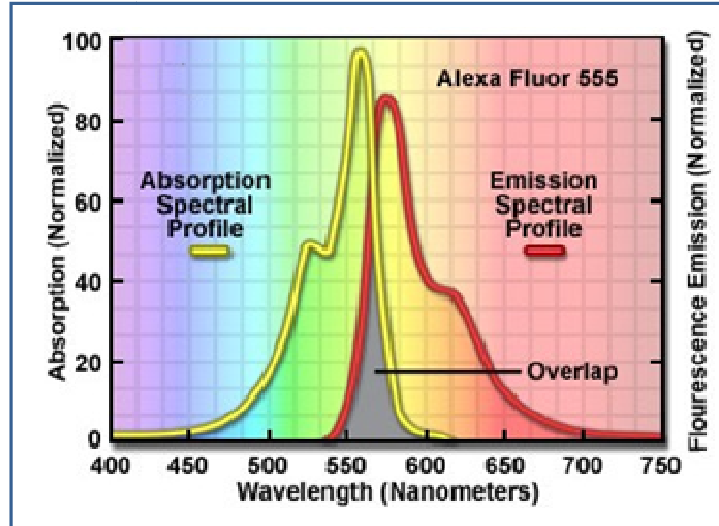


Figure 1.3 Stokes Shift
©Nikon Microscopy

comparing standard emission spectrum of fluorophores to the spectrum of the pixel. Thus, fluorophores can be used to detect multiple targets in a single specimen using hyperspectral imaging microscopy. For example co-expressions of receptors, such as Her-2, estrogen receptors (ER) and progesterone receptors (PR) commonly used in breast cancer diagnosis, can be simultaneously detected and quantified using these hyperspectral imaging microscopy systems.

1.3 Pseudocoloring

Pseudocoloring by definition means assigning arbitrary colors to its grayscale images. It is a powerful tool that can be used by a pathologist for diagnostic applications. Pathologists routinely use various dyes to stain tissue samples to study the behavior and structure of cells. Using dyes as contrast medium, pathologists try to identify changes in cellular constituents to correlate it to diseases or abnormality conditions [6]. An unstained tissue sample is difficult to diagnose since its histological structures are colorless, making it difficult to differentiate various structures in them [figure]. Hematoxylin and eosin (H&E) staining protocol is routinely used by pathologist to investigate the various histological structures of the sample with distinguishing

colors [6]. Hematoxylin stains the nuclear region from blue to purple while Eosin dye stains the cytoplasm and connective tissues from pink to red [6]. Although these dyes have affinity for the cellular constituents they are non-specific. It is also difficult to quantify and assess the extent of involvement of individual dyes within single compartment of cell. Though effective, this is a subjective method hence varies from one pathology lab to another. This method is thus ill-suited for quantification and reproducible assessment of tissue structures and also limits the standardization of staining protocols. Using hyperspectral imaging it is possible to obtain images with spectral signatures from an unstained tissue sample. Knowing the standard emission spectrum of various cellular structures it is possible to perform image segmentation of the composite image. Using these standard spectral signatures we can identify and assign arbitrary colors to various cellular structures within single cell. This technique is known as digital staining or pseudocoloring. It allows displaying the unstained tissue sample to resemble a stained tissue sample. Pseudocoloring using hyperspectral imaging microscopy is an extremely powerful tool that can be applied to pathology. Its use in pathology not only standardizes results but also allows the pathologist to re-analyze the same unstained tissue sample with a different protocol, if need be, without actually staining it.

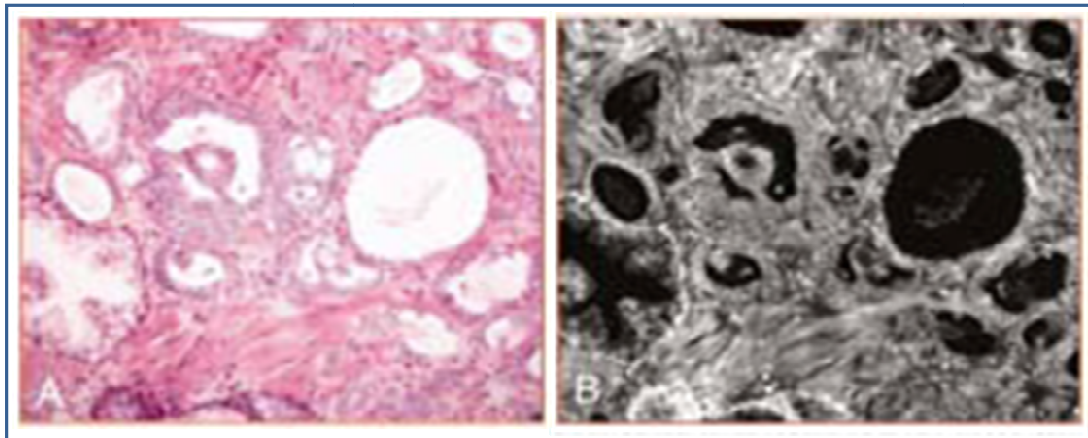


Figure 1.4 H&E Stained Tissue Sample and an Unstained tissue sample
©Richard Levenson, CRI Inc.

1.4 Research problem

The primary goal of this thesis is to design and develop software logic to control individual hardware components of hyperspectral imaging microscopy and display resultant X-Y image with spectral information. Next, this software aims to provide performance evaluation of hyperspectral imaging system by demonstrating precise quantitative measurements of multiplexed fluorophores on a variety of pathology sample types. We hypothesize that pathology can be revolutionized through the use of hyperspectral imaging microscopy (HMI) by making the measurement of highly multiplexed fluorophores, and through the development of methods to display unstained tissue sections with artificial coloring that resembles the view of stained tissues. This thesis work also aspires to investigate the heterogeneity in the intensity of staining of the clonally derived cells lines [skip garner]. Further down, it aims at correlating the HMI intensity number of each tumor marker with conventional subjective 0-3+ analysis. This aims to provide quantification of expression levels of tumor markers determined by pathologists [skip garner].

CHAPTER 2

METHODS

In this chapter we will discuss, the instrumentation of hyperspectral microscopy imaging system (HMI) with a great detail. The specifications of the hardware components of this system are also included in this. It is then followed by a description of the application software developed for exploiting the various parameters of the hardware components used in HMI. Furthermore, it discusses integration of all these features for accurate image acquisition, display and analysis of the resultant X-Y images.

2.1 Hyperspectral Imaging Microscopy System

Hyperspectral imaging microscopy system (Figure2.1) consists of a standard epi-fluorescence inverted microscope, an imaging spectrograph, a stage motor and a charge coupled device (CCD) camera. The inverted microscope allows us to record information about the current state of the cells at a desired magnification. Depending on the purpose of the application multiple illumination sources can be used with the microscope. The different sources that can be used are helium neon laser, argon laser, 532nm solid state laser or a100W mercury and xenon arc lamp laser. The microscope is also equipped with a objective lens of power 40X Plan Apochromat Dry or 60X/100X Plan Apochromat Oil and a set of standard filter cubes such as U-MWU, U-MWIB. The microscope is equipped with the micro-mover stage motor that moves the sample slide across microscope objective lens. The light emitted from the sample is positioned onto an imaging spectrograph which disperses the emitted light into its components.

The light emitted from the sample is positioned on the spectrograph through its narrow entrance slit. This narrow slit is optically coupled with the side port of the microscope and permits only a single line of an image. The size of this single line image depends on the ratio of the objective lens and the slit width used for the HMI system. The light components dispersed by the spectrograph are then focused onto a CCD camera. HMI records this information and then transfers it to a computer in binary format.

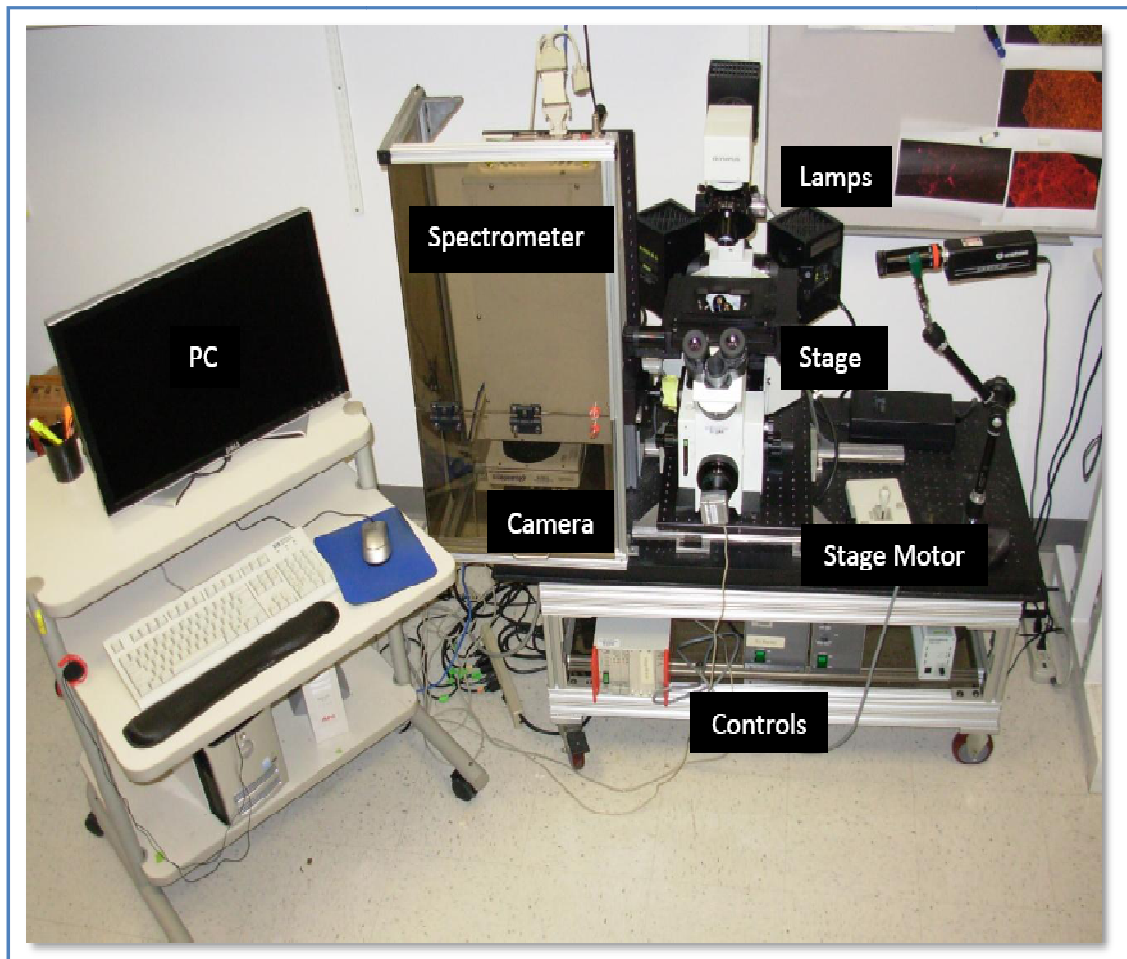


Figure 2.1 Hyperspectral Imaging Microscopy System

2.1.1 Epi-Fluorescence Microscope System

One of the most important components of the HMI system is the epi-fluorescence inverted microscope, Olympus IX70 (Figure 2.2). In this inverted microscope, its objective lens and filter turret are situated below the stage of the microscope which holds the specimen slide. This allows live cell fluorescence imaging of target cells possible. Various excitation sources such as lamps and lasers can be used with this assembly to visualize cells stained with various dyes.

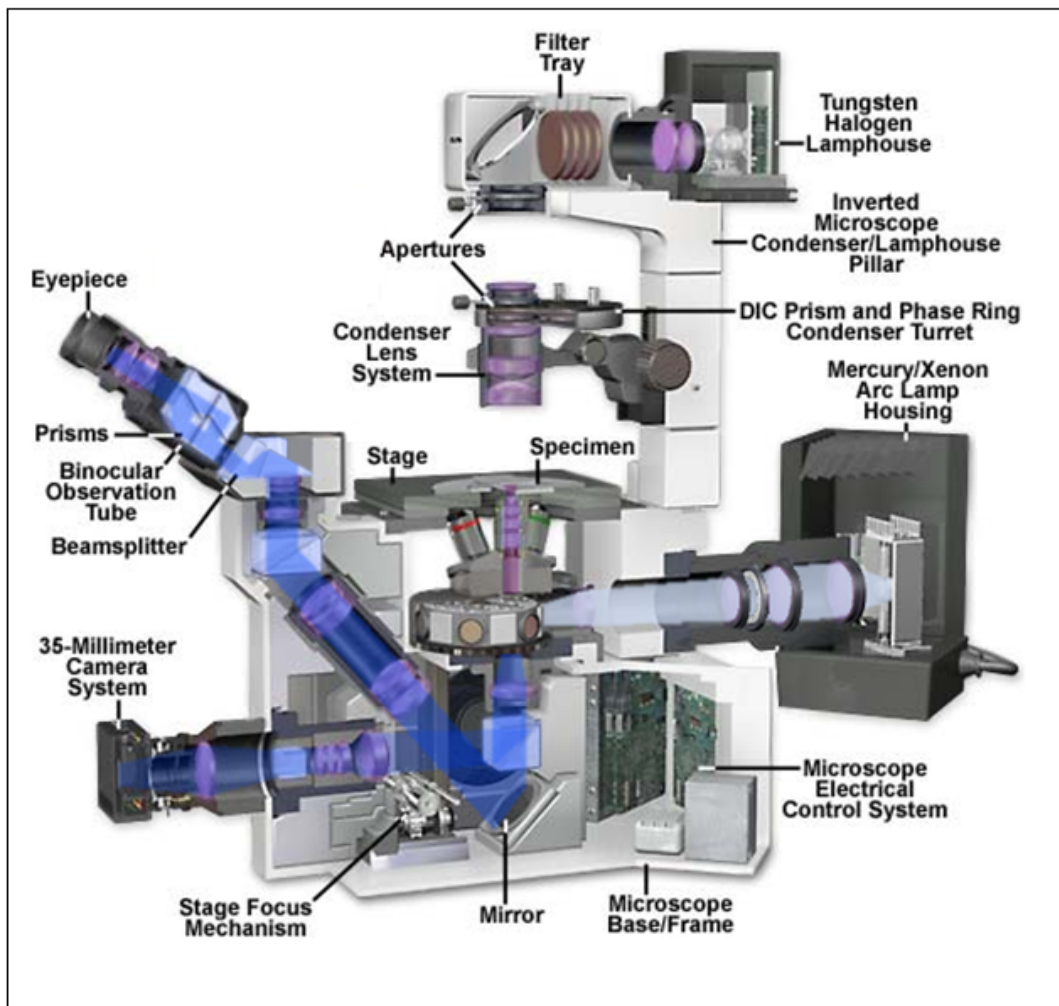


Figure 2.2 Schematic Cut Way Of Olympus Ix Epi-Fluorescence Inverted Microscope
©Olympus microscopy center

Illumination sources such as mercury arc lamp or xenon arc lamps are used in the HMI system. These sources emit constant polychromatic white light in visible spectrum (400-800nm) range as shown in figure 2.3 and figure 2.4 thus providing appropriate excitation for visible range applications. This constant illumination white light provides precise excitation wavelengths for fluorescence emission of target molecules within the cells. Accordingly, filter cubes (Figure 2.5) with dichroic mirror and excitation and emission filters are used to select a band of excitation wavelengths. These excitation filters allow only a selected band of wavelengths, from the illumination source, to pass through the filter cube onto the objective lens of the microscope [24]

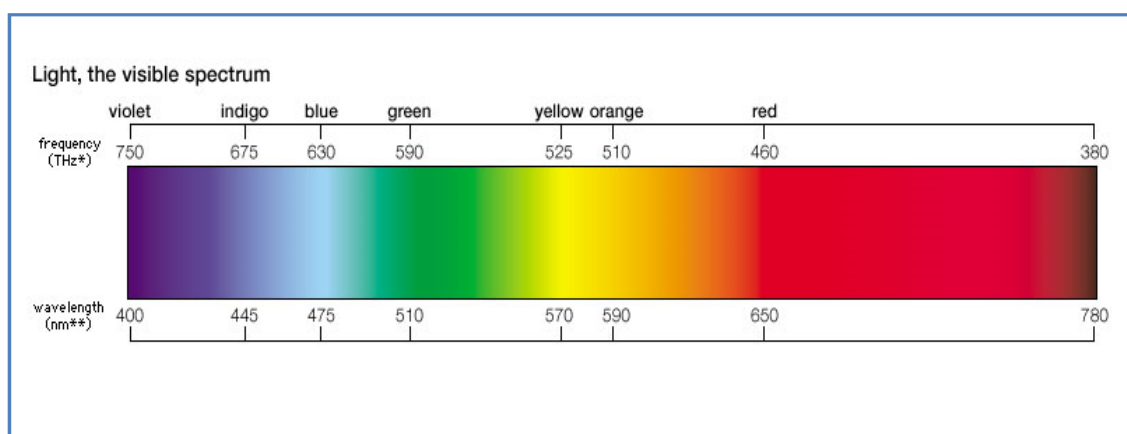


Figure 2.3 Spectrum of Polychromatic White Light in Visible Range
©Encyclopedia Britannica Inc.

The barrier filter suppresses or blocks the excitation wavelength and allows only the emission wavelength to pass towards eyepiece or detector [24]. Dichromatic mirrors on the other hand are designed to efficiently reflect excitation wavelengths and only pass the emission wavelengths to an eyepiece or the camera port [23]. For applications in the visible range, HMI uses U-MWU and UMWIB filter cubes. The excitation filter range of the U-MWU filter cube is 300-385nm and it acts like a long pass filter starting at 420nm, as indicated by the Table 2.1 below. It can hence be said that the U-MWU filter cube operates entirely in the visible range [6]. On the other hand the U-MWIB filter has excitation in range of 460-490nm and acts as a long pass filter starting at 515nm.

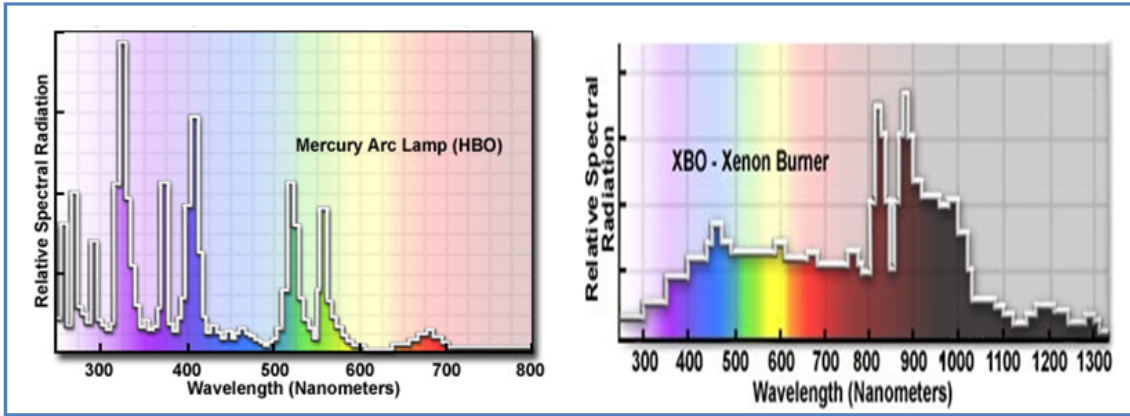


Figure 2.4 Emission Spectrum of Mercury and a Xenon Arc Lamp in the visible range
©Olympus microscopy center

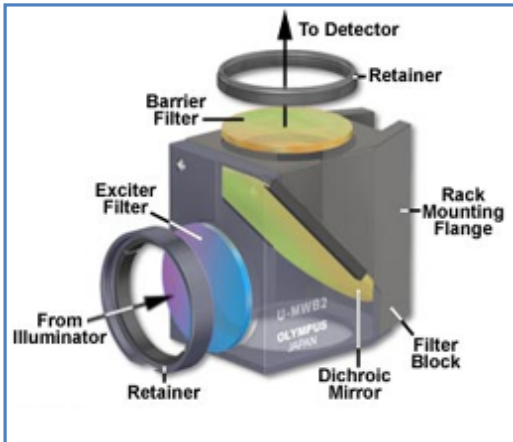


Table 2.1 Filter Cube Specifications
©Olympus microscopy center

Filter cube	U-MWU	U-MWIB
Excitation filter (nm)	300-385	460-490
Dichroic mirror(nm)	400	505
Barrier filter(nm)	>420	>515

Figure 2.5 Standard Filter Cube
©Olympus microscopy center

Thus U-MWIB filter cube can only be used to record wavelengths above the green wavelength. This feature of the U-MWIB filter cube is very useful in viewing the cytokeratin in the epithelial tissues [24]. This is because the cytokeratin is usually conjugated with green fluorophores (AF488) [24].

The high intensity polychromatic white light then reaches the target specimen slide through

microscope objective lens and excitation/barrier filter. The objective lenses are responsible for proper image formation and also provide appropriate image magnification. It enables us to view the finer details of the microscopic structures. The light emitted, by the fluorescently labeled cell structures, passes through this objective lens and an emission filter of the filter cube. The image formed through permitted band of emission wavelengths can then be seen through an eyepiece or focused onto an exit port for recording this information. In order to distinctly image cellular components of a few microns a 60X magnification objective lens is used in the HMI system. An imaging spectrograph optically coupled with the exit port of microscope disperses the emitted light into its components. This spectrograph would provide spectral information about the image.

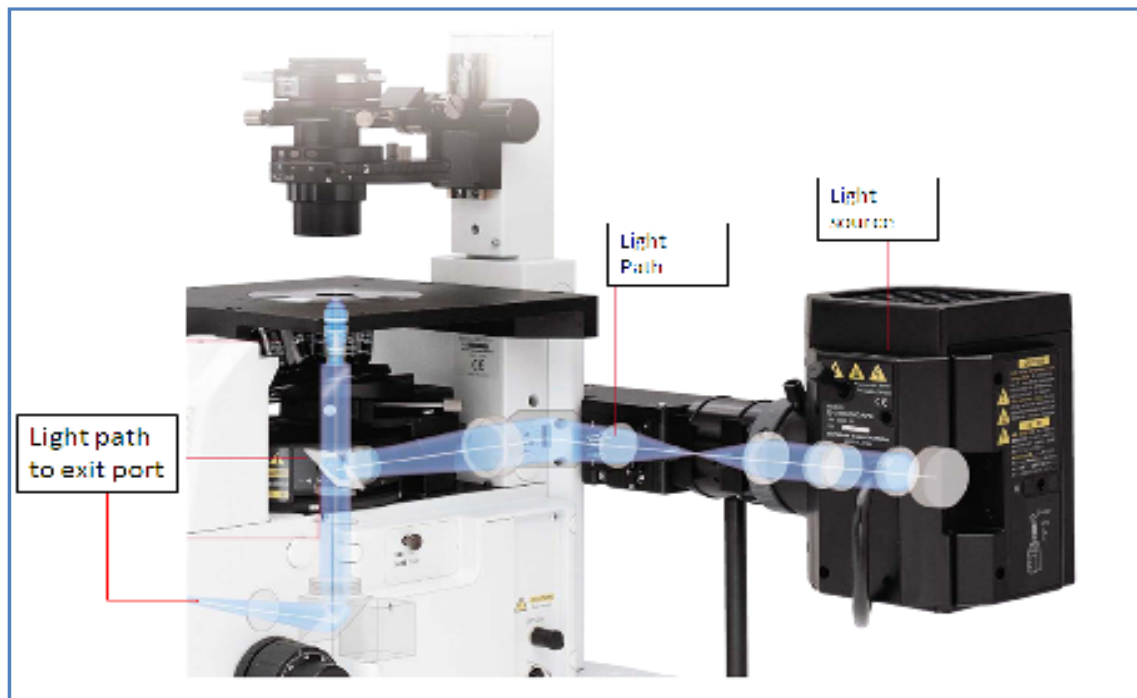


Figure 2.6 Optical path of Illumination Source through the Microscope
©Olympus microscopy center

2.1.2 Imaging Spectrograph

A Spectra Pro 500i imaging spectrograph from Roper Scientific is optically with microscope through its narrow entrance slit. This spectrograph uses diffraction principle to separate polychromatic "white" light into its individual wavelengths. Each of these individual wavelengths is seen at slightly different angles [Figure2.7].

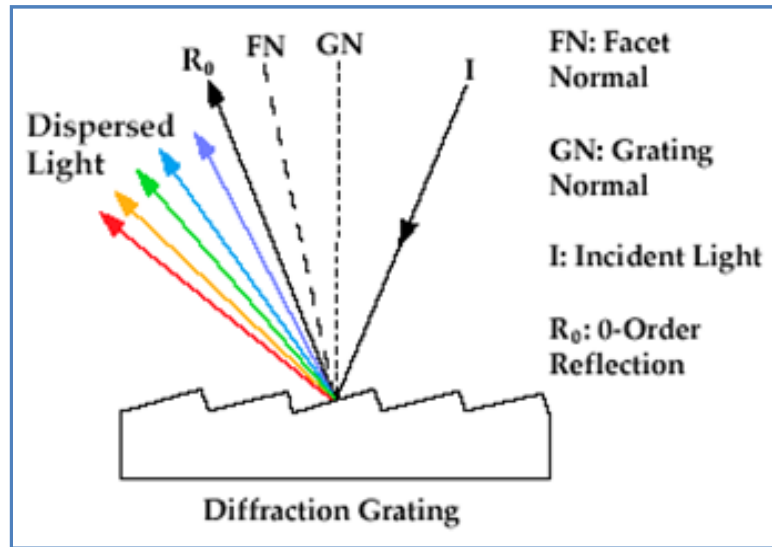


Figure 2.7 Typical Dispersion Grating in Imaging Spectrograph
©Photometrics

The monochromator or spectrograph focuses the dispersed light onto the detection system such as a CCD camera to record the information. The Spectra Pro500i imaging spectrograph is a triple grating spectrograph with focal length of 500 mm, aperture ratio of f/6.5, scan range of 0 to 1400nm and dispersion of 0.359 nm/pixel. It also has a CCD mounting at its exit port [2]. Depending on the range of the application i.e. the visible, IR or UV range the spectrograph gratings can be varied. The three gratings mounted on the spectrograph are 50, 80 and 100 groves per millimeter. The number of groves, on grating, affects mechanical scanning range and dispersion properties of the spectrograph



Figure 2.8 Similar looking Spectra Pro 500i Spectrograph

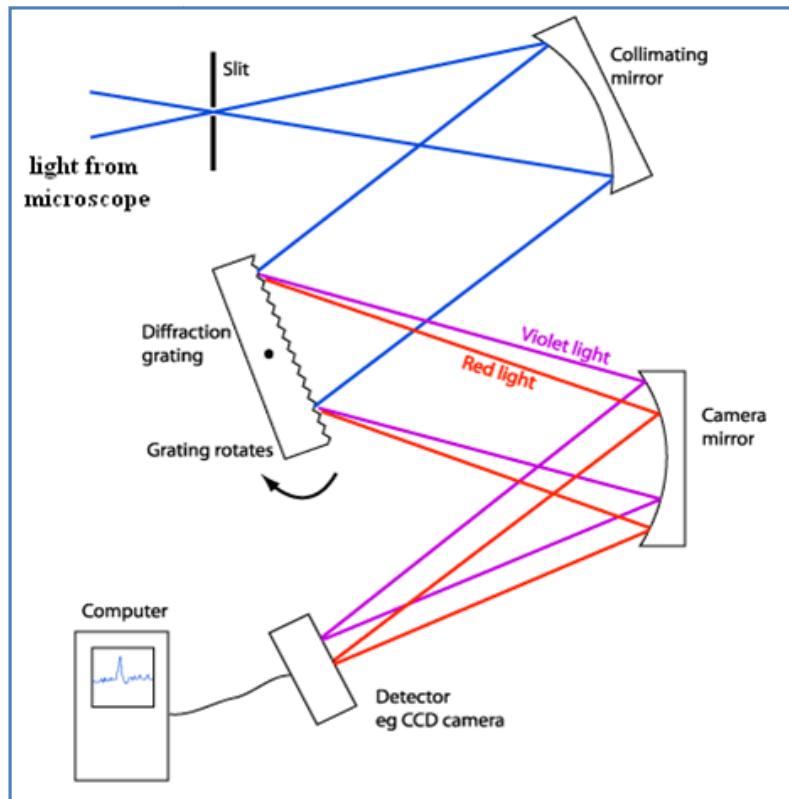


Figure 2.9 Schematic Working of imaging spectrograph

The HMI system uses Spectra Pro500i with 50 groves per millimeter blazed at 600nm. This allows making measurements in 400-780nm visible range possible. The narrow slit entrance of the spectrograph limits the light entering in the spectrograph. This act as like a point source of the light from a larger image being scanned [csiro.org]. This narrow slit has an adjustable width and its intensity response for 50 groves per mm grating is as shown in Figure2.10.

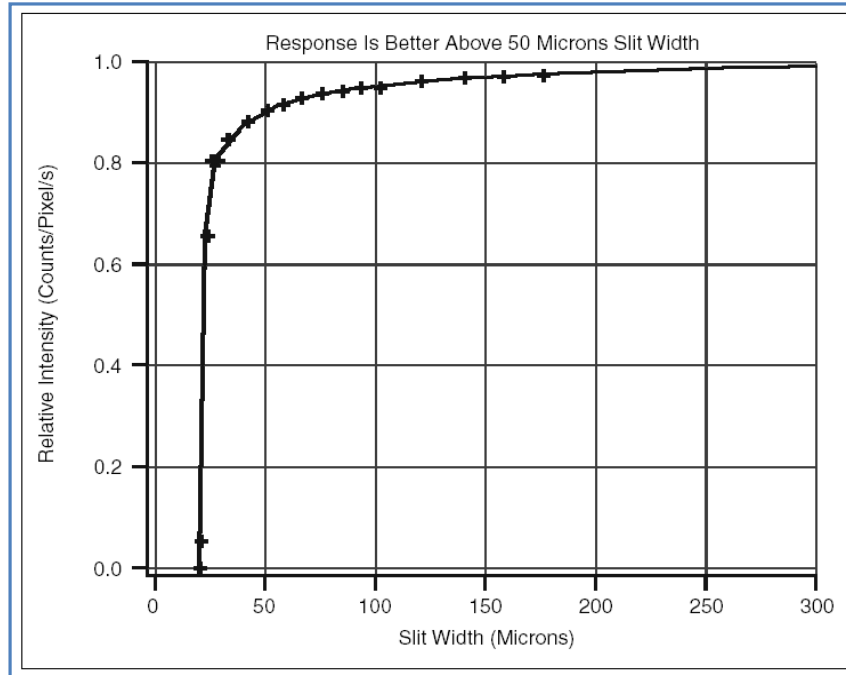


Figure 2.10 Relative Intensity Response to Spectrometer Entrance Slit Width
©Michael Huebschman

As observed, at 50 μm slit width approximately 90% of illumination light transmitted to spectrometer will reach the detector at exit port of the spectrograph. In order to obtain the best transmittance resolution the slit width in the HMI system is placed at 72 μm . This narrow slit width affects the spatial resolution of the resultant X-Y image. For HMI experiments Y direction corresponds to the long axis of the slit width and X direction corresponds to the slit width[2]. Thus in the Y direction the spatial resolution is affected by factor of pixels binned in Y direction and microscope objective power. While in X direction spatial resolution is affected by a factor of microscope objective power and the slit width of the spectrograph.

Binning is simply a process of merging adjacent pixels and is explained later in the Chapter. For example, an image with pixel size $9 \times 9 \mu\text{m}$, objective lens of 60X and slit width of $72 \mu\text{m}$ with 2 pixels binned in Y direction and 8 pixels binned in X direction. The image will then have $0.3 \mu\text{m}$ spatial resolution in Y direction and $1.2 \mu\text{m}$ spatial resolution in X direction. The point source of light from imaging spectrograph, along with its individual wavelengths is recorded onto the CCD camera. A number of spectra from different regions of an image can be thus captured and recorded onto a camera by stepping across the slide using the micro-mover stage.

2.1.3 Stage Motor

A stepper motor driven micro mover stage motor from the Ludl Electronics Products Ltd. (LEP) is used to precisely control the microscope position. This stage motor is fully automated through the controller, MAC2000 from Ludl Electronics and is connected using the RS232 interface. This micro-mover stage has two axis motors to control the movement in X-Y direction and the end points of this motor act as mechanical limit points in each of the directions. The LEP stage

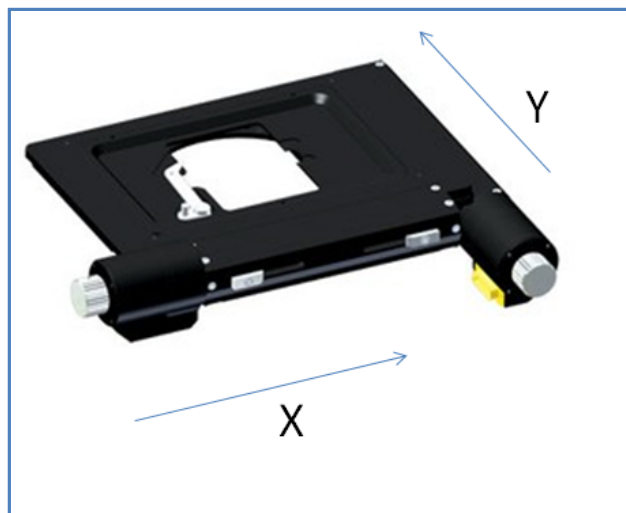


Figure 2.11 Schematic Working of X-Y Stage Motor

can move at a maximum speed of 30mm/sec. The speed of stage is software controllable and it is discussed later in the Chapter. The stage can be centered or moved precisely to a particular position using application software and its library functions. This micro-mover stage can also be manually controlled by using a joy stick [Figure2.12]. Joy stick allows to manually position the stage to a given location. It proves very helpful to quickly move the stage to find a region of interest in the specimen slide. Stage movement plays an important role in capturing the spectra from different region of an image. Although spectrograph acquires a complete spectrum at each acquisition it needs to step across the slide to cover the full spatial resolution of the image [5].

The micro-mover stage helps to achieve this by precisely and reproducibly positioning the slide to the next adjacent position without overlapping adjacent images [2]. This individual image when merged together builds a hyperspectral data cube. Thus, using the micro-mover stage and the spectrograph, one can acquire spectral and spatial information which can then be recorded using a CCD camera.

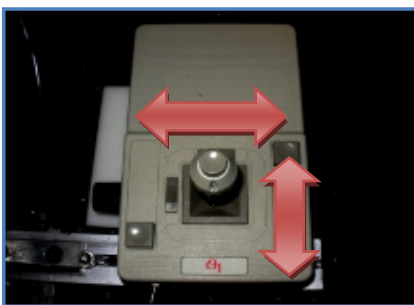


Figure 2.12 A Typical Joy Stick for manual control of the micro-mover LEP stage

2.1.4 Charge Couple Device (CCD) Camera

The output from a spectrograph is recorded by using a high resolution Quantix 1602E air cooled CCD camera system. Some of the specifications for the Quantix 1602E camera are as given below in Table 2.2. **Programmable Virtual Camera Access Method (PVCAM)** is a high

level C library used for such camera control and data acquisition functions [pvcam 2.6]. It provides an interface that allows specifying the camera's setup, exposure, and data storage attributes. The Quantix camera operates optimally between 0-30°C and generally lower temperature enhances the quality of acquired signal [photometrics]. The low light applications of fluorescence microscopy show a change in fluorescence properties with slight change in the surroundings. In such applications the high speed focus along with high resolution image capture is an absolute necessity.

The camera provides high frame readout speeds of 1MHz or 5MHz. Such high speeds allow high speed focus and image capture. It can also capture full frame in 0.35sec only at 5MHz frame readout speed. To provide quantitative results, high precision and high sensitivity data the camera is provided with a 12 bit digitization range. Along with 12 bit digitization range the camera provides pixel array of 1536X1024 pixels. Each of these pixels is 9X9 μm in size; such small pixel size along with large pixel array provides high spatial resolution.



Figure 2.13 A Typical Quantix 1602E air cooled CCD Camera

Table 2.2 Typical Quantix 1602E CCD Camera Specification Sheet

Specifications	
CCD Format	1536X1024 imaging array 9X9 μm - pixel pitch 13.8X9.2 mm imaging area (optically centred)
Well Capacity	167,000 e ⁻ @ 0.5X 86,000 e ⁻ @ 1X 20,000 e ⁻ @ 4X
System Read Noise	High Signal to noise ratio 37/37 e ⁻ rms@ 0.5X High dynamic range 25/25 e ⁻ rms@ 1X High sensitivity 16/16 e ⁻ rms@ 4X
Nonlinearity	$\leq 0.5\%$
Dynamic Range	12 bits @ 5MHz Digitization
Frame readout	0.35 sec for 5Mhz
Dark current	0.05e ⁻ /p/s
Operating environment	0 to 30 ° C ambient
Dimensions	4.5" X7.2" 3 lb

In low light fluorescence microscopy applications every single photon is extremely important. It is thus necessary to ensure that the signal level relative to noise is adequate to allow capture of accurate image information. The 12 bit digitization rate provides a 12 bit monochrome digital image that has 4096 (since $2^{12}=4096$) distinct shades of gray. A high dynamic range is thus achieved because of the 12 bit digitization rate. This allows us to image the subtle details in the dark shadows and the bright highlights or the midtones [photometrics]. The dispersed light focused onto the camera, falls on the surface of the silicon chip and the corresponding electrons (electron charge) accumulates in each pixel [9]. The number of electrons that can accumulate in each pixel is referred to as its Well Depth. These analog electron charges are then swept off from the silicon chip to form the electrical impulses. These electrical impulses

need to be digitized in order to be displayed on the computer. An analog to digital convertor (ADC) is used provides this digitization. This converter in the CCD camera translates the analog impulses or electron charges into the precise digital values which are then displayed on a computer thus producing an image.

This can be explained through an analogy shown in Figure 2.14, imagine a field covered with an array of buckets to collect the rain water. After a storm, the buckets are transported through a conveyer belt to a metering station. At the metering station the amount of rain water in each bucket is measured. Thus amount of rainwater collected in each different section of the field is measured. Correlating it to the CCD application, the buckets correspond to the pixels and the rain water collected corresponds to electron charges. When the ADC translates the electron impulses into the digital numerical values, the values are recorded in a simple binary code for the computer.

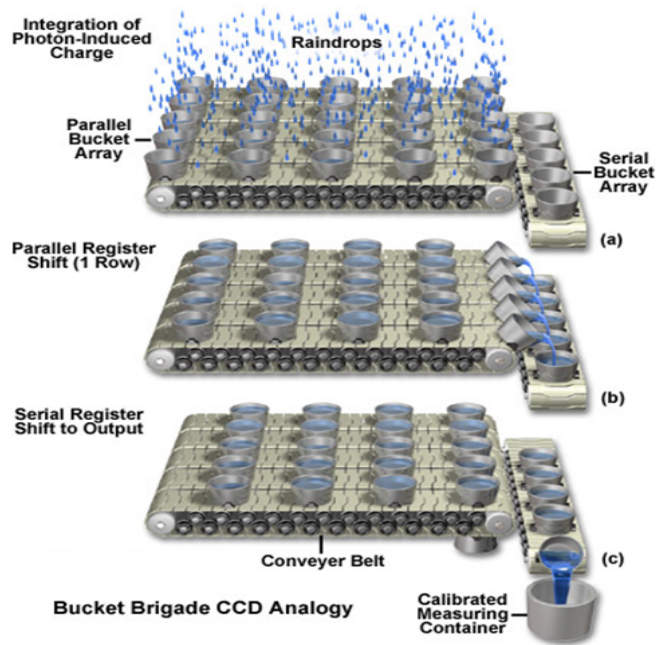


Figure 2.14 Analogy for Charge transfer in a Typical CCD Camera
 a: the pixels of CCD collect light and convert it to packets electrical charges
 b: the charges are quickly moved across chip
 c: the charges are then swept off the CCD and converted into electrical impulses

The quality of the signal received by the ADC is a determining factor for the image resolution. If the ADC receives a high-quality signal, the 12-bit ADC digitizes the analog signal into 12-bit data. With a lesser quality signal, the ADC produces data with a lower effective bit depth. The KAF-1602 silicon chip used in the Quantix 1602E CCD camera has a maximum well depth 85,000 electrons [Kodak]. In the CCD camera, the gain refers to the magnitude of amplification that will be produced in the system [photometrics]. By default, the gain of the camera is typically set so that the full well of the CCD matches the full range of the digitizer (at 1x gain). The camera's gain can also be selected using PVCAM library to meet the needs of a given application. Through software control, the camera can be set to the 3 basic gains settings listed below.

High Signal-to-Noise Mode (Gain 1) – when binning, this mode takes advantage of the output node's maximum full-well capacity which is a requirement when measuring small changes on bright backgrounds. In this mode (1/2x), the full well of a normal pixel maps to 1/2 of the maximum ADC count [photometrics].

High Dynamic Range Mode (Gain 2) – this mode is suitable for measuring bright and dim signals in a field of view. In this mode (1x), the full well of a normal pixel maps to the maximum ADC count [photometrics].

High Sensitivity Mode (Gain 3) – this mode takes advantage of the CCD's low read noise, a

Table 2.3 Quantix 1602E CCD Camera Gain Specifications
©Photometrics

Detection Mode	Gain Setting	Relative Gain	Typical Noise	System Gain	Typical Maximum ADC Signal
High Signal to Noise	1	≈1/2x	26e ⁻	≈40e ⁻ /ADU	160Ke ⁻ (binned full well*)
High Dynamic Range	2	≈1x	19e ⁻	≈20e ⁻ /ADU	80Ke ⁻ (single pixel full well)
High Sensitivity	3	≈4x	11e ⁻	≈5e ⁻ /ADU	20Ke ⁻ (high sensitivity)
* Binning must be a minimum of 2 pixels in the parallel and serial direction to reach the maximum ADC signal.					

requirement for low-light imaging. In this mode (4x), 1/4 full well of a normal pixel maps to the maximum ADC count [photometrics].

The HMI system uses gain 3 setting for its low light fluorescence based experiments. Another important factor of the CCD camera is its quantum efficiency. Quantum efficiency measures the effectiveness of an image to produce electronic charge from the incident photons. This is

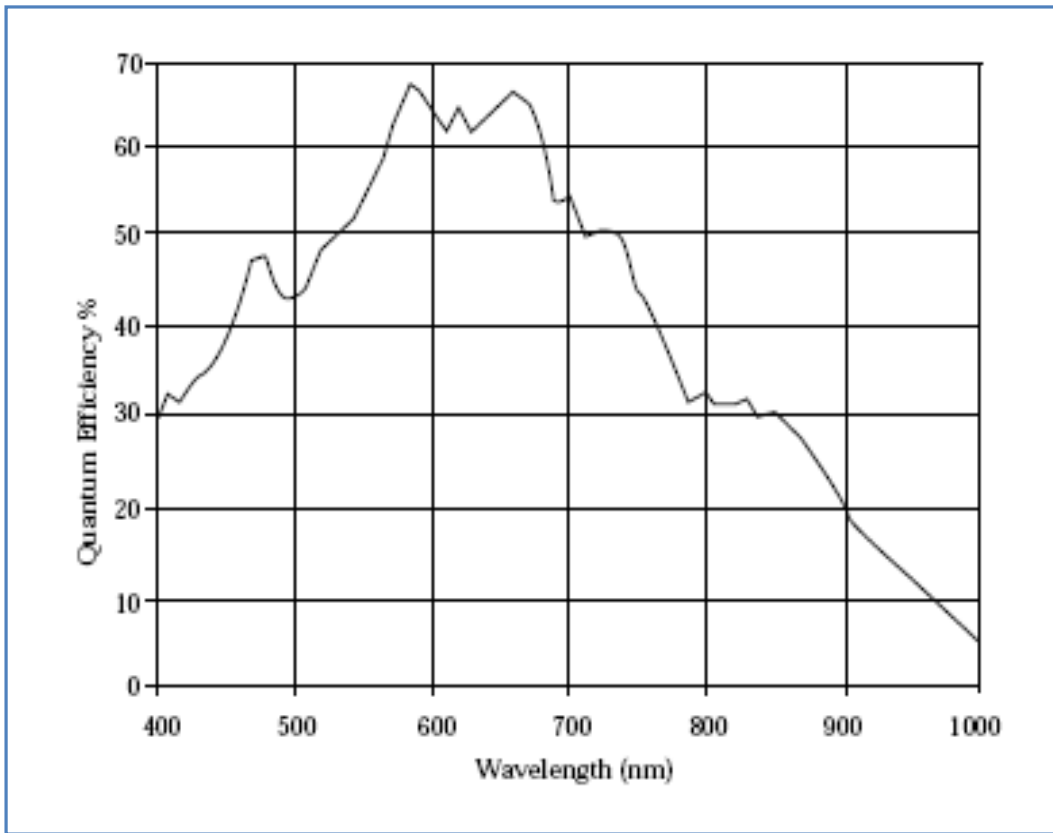


Figure 2.15 Quantum Efficiency for Quantix 1602E CCD Camera
©Photometrics

especially an important property when performing low-light imaging and examining properties of the elements or the way the elements interact with light. Spectral response of the camera shows that its maximum quantum efficiency is 66% in 600-700nm range. The quantum efficiency is above 55% for all our visible range applications in wavelength range of 400-780nm, and at no point it goes below 30% within this range.

Saturation and blooming are phenomena that occur in all the CCDs and affect both the quantitative and qualitative characteristics of imaging. If each individual pixel can be thought of as a well full of electrons, then saturation refers to the condition where the well becomes completely filled. At saturation, pixels lose their ability to accommodate additional charge. This additional charge will then spread into neighboring pixels, causing them to either report erroneous values or also saturate. This spread of charge to adjacent pixels is known as blooming and appears as a white streak or blob in the image. The dark noise arising due to statistical variations of thermally generated electrons within CCD is another important parameter to control. The Quantix CCD camera reduces this dark noise by cooling CCD with a thermoelectric cooler [8] at the hardware level.

2.1.4.1 Binning

Binning is the practice of merging charge from the adjacent pixels in a CCD prior to digitization. The on-chip circuitry of the CCD allows binning by controlling the serial and parallel registers of the CCD array. Binning helps to reduce the readout time, save computer memory and increase the signal to noise ratio but affects the image resolution. Binning process increases the focusing accuracy by reducing the time necessary for the image acquisition. It also provides greater sensitivity to lower out-of-focus light levels. In a typical CCD the charge transfer is accomplished in two steps [Figure2.16]. In the first step, an entire row is shifted in the vertical direction. In the second step, this uppermost row is shifted serially in the data register and then

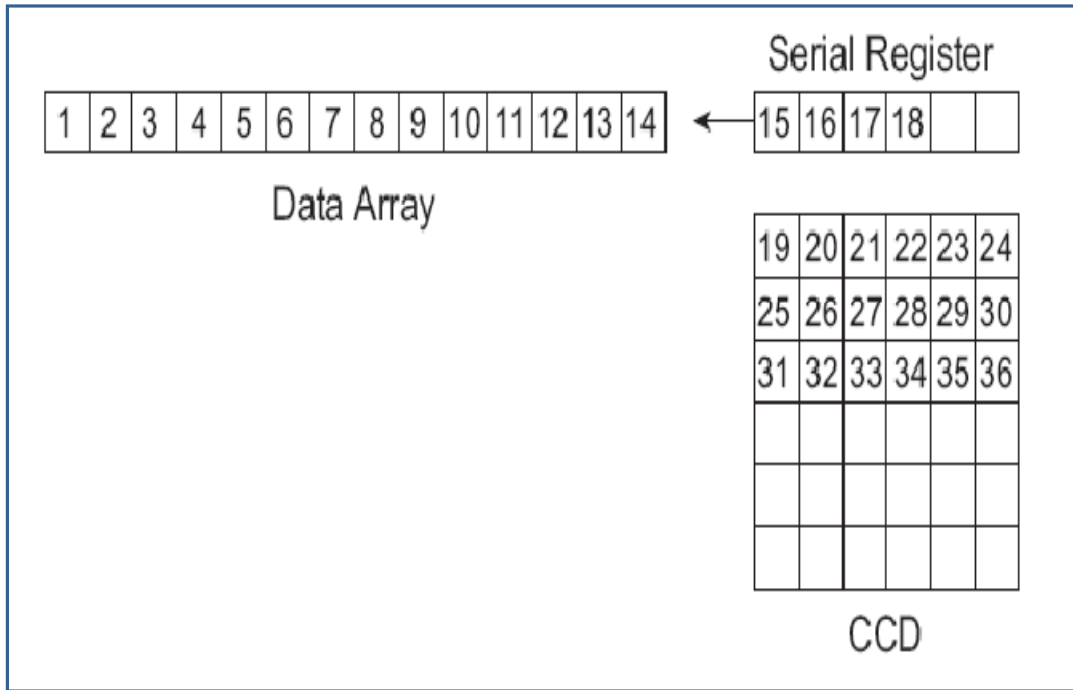


Figure 2.16 Schematic of a Typical Charge Transfer in a CCD Array

to the output amplifier. To comprehend the binning practice in the scientific cameras, consider the examples shown below in Figure 2.17 and 2.18. Binning 1x1 where no charges are summed provides us the maximal resolution. Figure 2.18 shows the CCD at the end of an exposure. The capital letters represent different charges accumulated on the CCD pixels. Readout of the CCD begins with the parallel readout phase, Figure 2.17 (2), simultaneous shifting of all pixels in a bottom row towards the serial register followed by the serial readout phase, Figure 2.17 (3) and Figure 2.17 (4). The charge in the serial register then shifts into the summing well which is then digitized. Only after all the pixels in that particular row are digitized, is the second row from the bottom moved into the serial register. Thus for example above, the order of shifting is therefore A1, B1, C1, D1, A2, B2, C2, D2, and A3.... and so on [10].

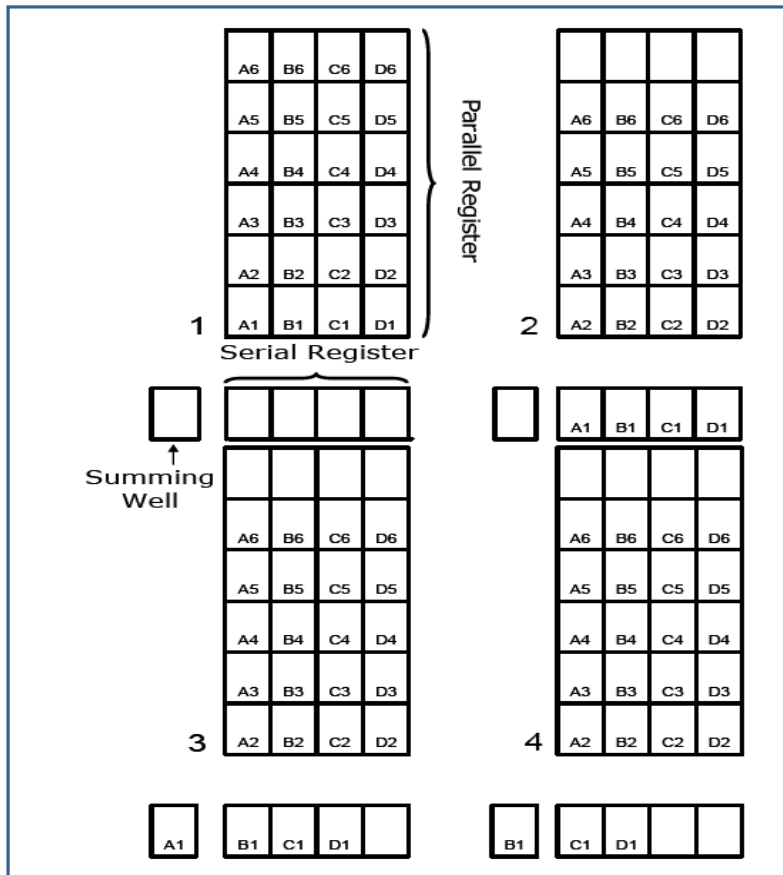


Figure 2.17 A Typical Frame Readout for 1X1 Binning process

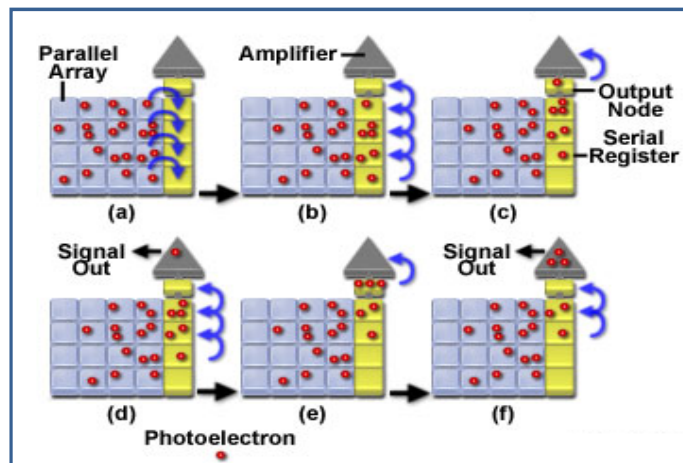


Figure 2.18 Schematic of the charge transfer for 1X1 binning in a CCD Camera

A binning of 2x2 means that an area of 4 adjacent pixels has been combined into one larger pixel. The charge that has been integrated during the exposure is shown as capital letters in Figure 2.19 (1). Readout begins with a parallel readout as shown in Figure 2.19 (2). Since binning of 2 x 2 is required, charge from two rows of pixel, rather than a single row during 1 x 1 binning, is shifted into the serial register. The charge is then shifted from the serial register, Figure 2.19(3) and Figure 2.19(4), two pixels at a time, to the summing well rather than a single pixel as in binning 1 x 1.

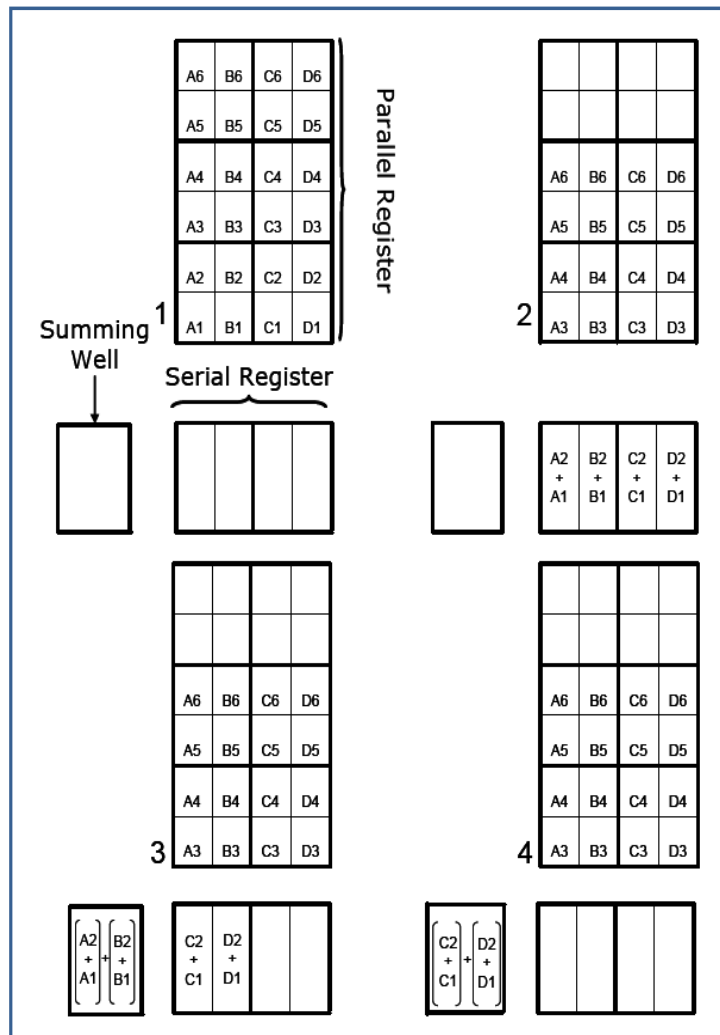


Figure 2.19 A Typical Frame Readout for 2X2 Binning process

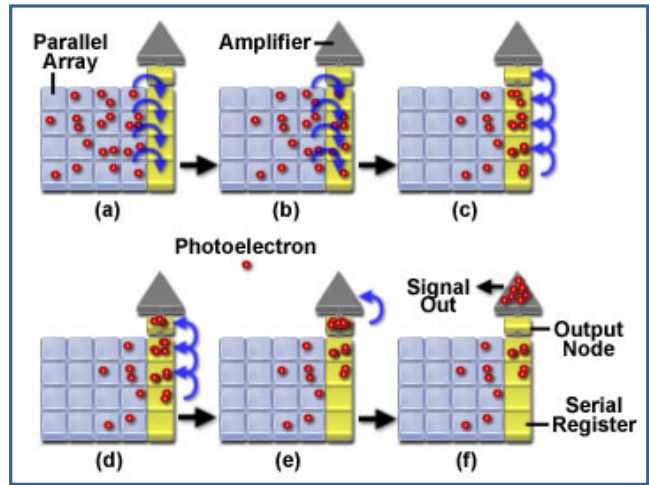


Figure 2.20 Schematic of Charge transfer for 2X2 binning in a CCD Camera

Binning can be a very useful tool. It can be used to effectively increase the pixel size while also increasing the sensitivity. It is a good method for focusing, because the image acquisition speeds up greatly. Along with this, greater sensitivity is also achieved. This helps in focusing lower out-of-focus light levels. The Quantix camera having 1536X1024 pixels with 9 μ m pixel pitch can appear to have 768X512 pixels with 18 μ m pixel pitch with a binning of 2x2. With 3x3 binning, the sensor appears to have 512X341pixels with pixel pitch of 27 μ m [Figure2.21]. Binning factor is software selectable and is programmed at default of 2X2 binning factor. This 2X2 binning provides 768X512 pixels with 18 μ m pixel pitch.

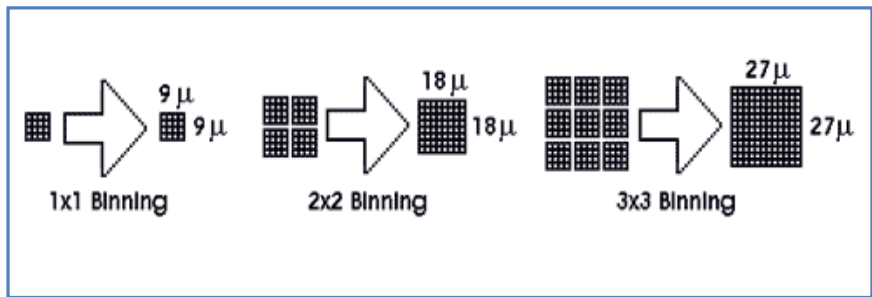


Figure 2.21 Typical Pixel binning
 © <http://www.ccd.com/ccd103.html>

2.2 Software

Hyperspectral imaging microscopy (HMI) integrates individual hardware components through Xanoscope®. Xanoscope® is application software developed using VC++ programming language. It provides a complete control over hyperspectral imaging system for precise data acquisition and automated control. Xanoscope® provides control over the 3 basic hardware components the CCD camera, the spectrograph and the micro-mover stage. The basic flow chart of HMI system is shown in Figure 2.23. On running the Xanoscope®, HMI system gets initialized and updates the hardware components with its default parameters. The user can modify these parameters depending on experimental setup by browsing through the settings of individual hardware components. The system then starts the scanning procedure. After capturing the first image, the image is positioned on the spectrograph. Depending on imaging spectrograph's entrance slit width, only a single line of image is allowed through on to the focusing camera. During a scan Xanoscope® captures such individual single line pictures onto CCD camera. These individual pictures are captured along Y- λ plane and stage is moved incrementally in X direction to cover spatial resolution .



Figure 2.22 Xanoscope® application Software Splash Screen

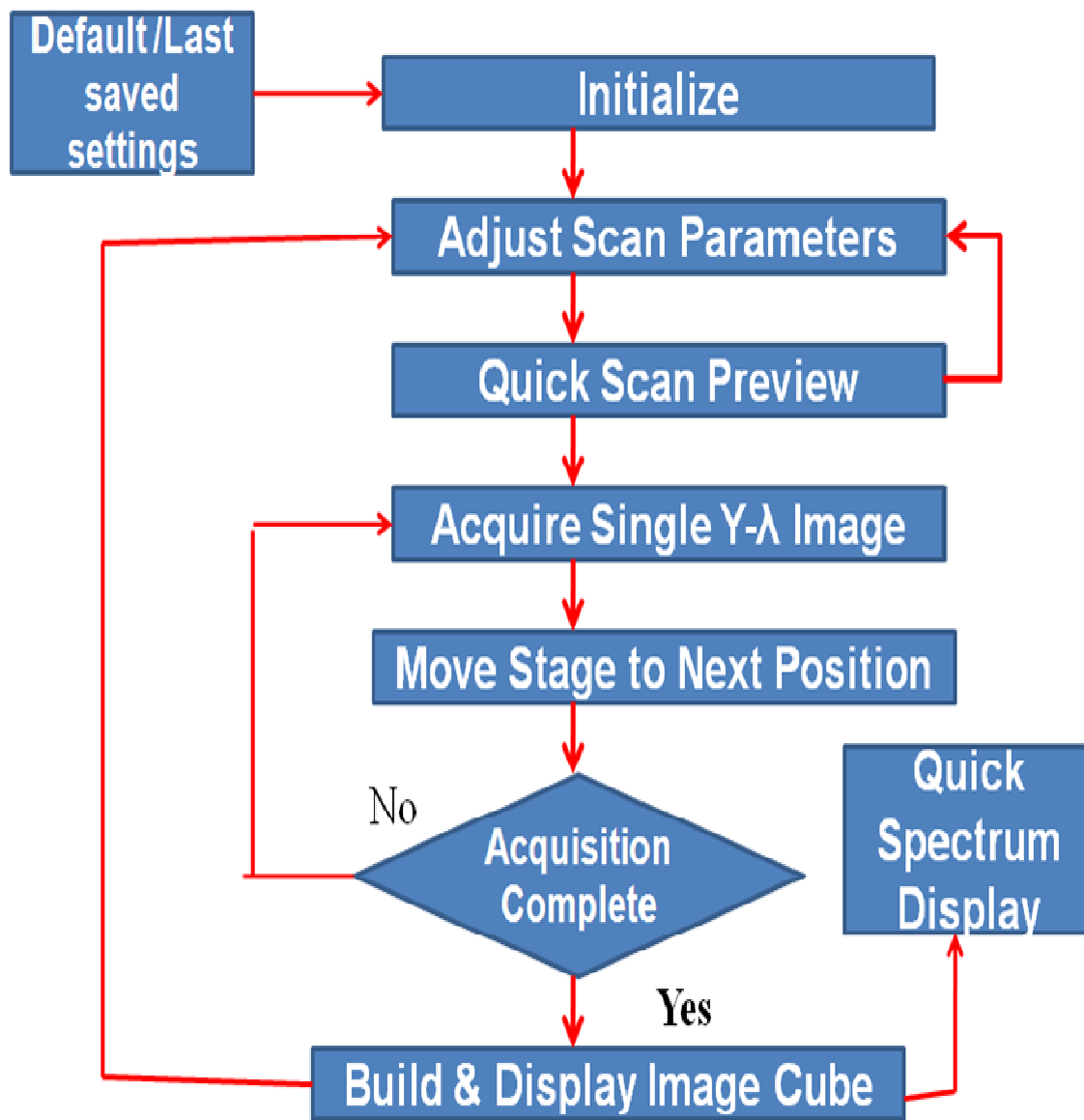


Figure 2.23 Flow Chart of Xanoscope®

This allows the hyperspectral imaging system to acquire wavelength as a component of two dimensional data plane [Figure2.24]. The Y- λ scan file is then stored into the user defined location as a text file. A stack of such Y- λ raw data files from the image are then added together to build a hyperspectral image cube [figure2.24]. Thus, the image cube developed would

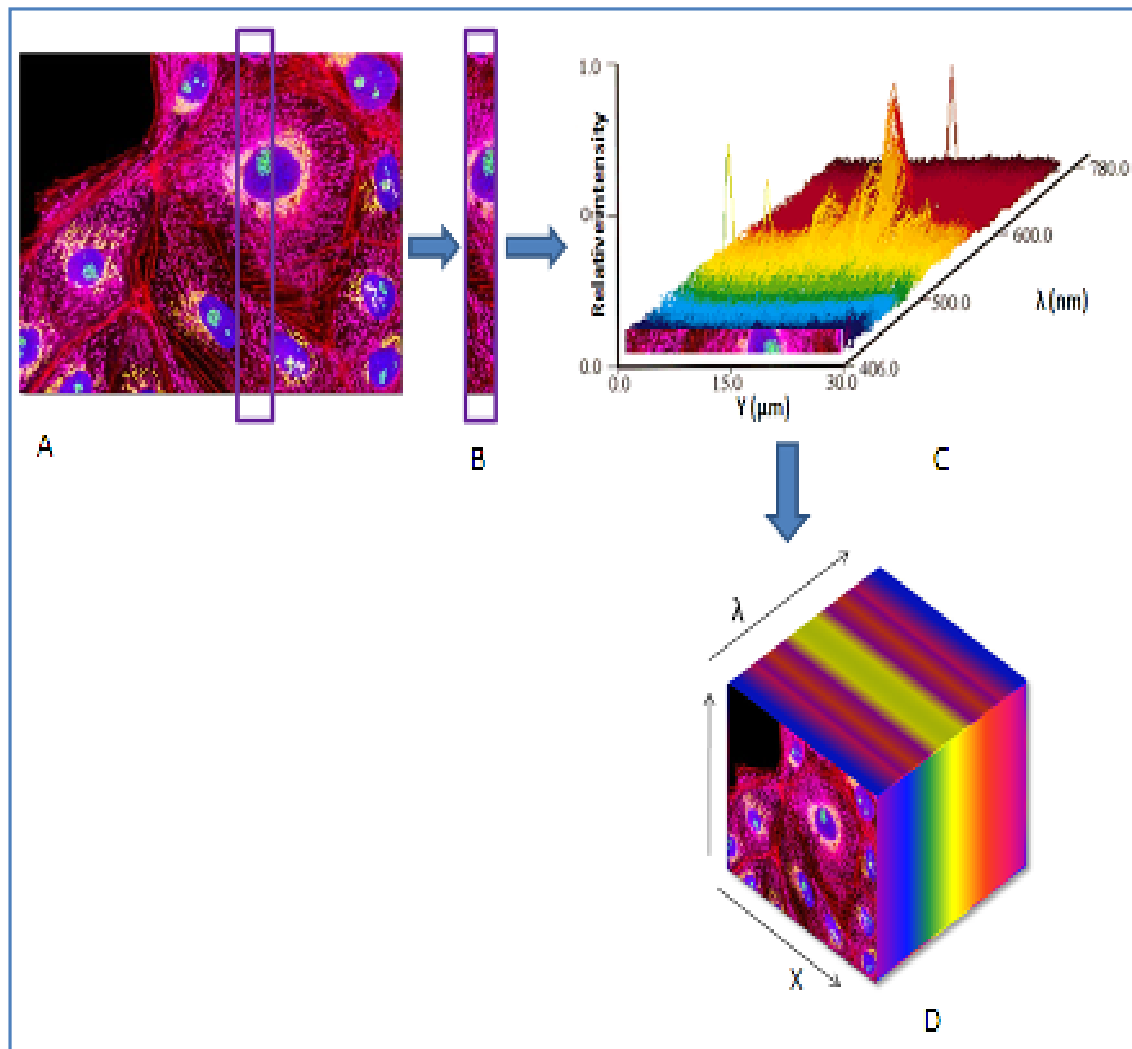


Figure 2.24 Schematic of Construction of a typical Hyperspectral Data Cube
A: Typical target specimen to be scanned
B: A Single line Y- λ slice as focused on to detector port of spectrograph
C: A Single Y- λ line with allied spectrum for each pixel in image
D: Hyperspectral Data Cube

display resultant X-Y plane. Spectral decomposition of these raw data files can be performed to obtain emission spectrum for any pixel in that X-Y image.

2.2.1 Characterizing the Hardware

Individual hardware components can be initialized using various parameters, controlled by the Xanoscope®. The main window of Xanoscope® provides a user interface to browse through various options available to complete the scan procedure. This section further, explains various device parameters that can be modified for camera, stage and spectrograph depending on the purpose of the application.



Figure 2.25 Main Window of Xanoscope® Software

2.2.1.1 Camera

Xanoscope uses PVCAM library functions to provide complete control over the Quantix CCD camera. The camera settings dialog box in Xanoscope® provides an interface to the various camera parameters. It can be navigated by browsing through the Actions button on the main window of Xanoscope® [figure2.26].

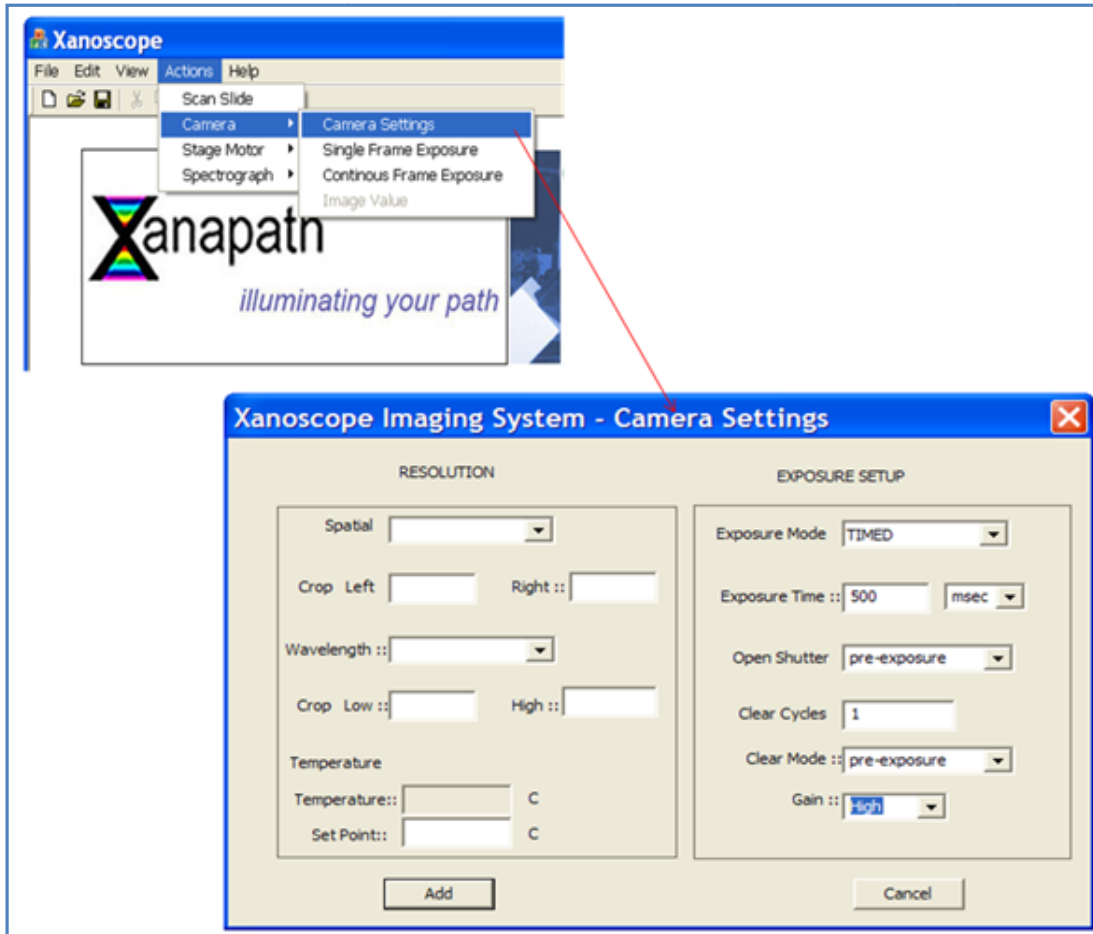


Figure 2.26 Camera Settings dialog Box of Xanoscope® to control various device parameters of Quantix 1602E CCD camera

Exposure time is one such parameter used to set. It is the time for which the CCD array is exposed to light. It is an important factor in determining the amount of light received by the CCD array. Longer exposure times are required for low light or dimmer background and very short

times for brighter backgrounds. Xanoscope allows exposure time to be set in seconds as well as milliseconds for very precise measurements.

During sequences, the exposure mode determines how and when each exposure begins and ends. Xanoscope provides six different exposure mode settings, TIMED MODE, VARIABLE TIMED MODE, TRIGGER FIRST MODE, STROBED MODE and BULB MODE. In timed mode, the duration of each exposure time as well as non-exposure time of the CCD array is constant throughout. Whereas for a variable timed mode this duration varies and only the time between two exposures remain constant. In trigger first mode, camera begins exposure only after external trigger pulse is given and then continues exposure sequence like in timed mode. In strobed mode, for every external trigger pulse an exposure takes place but each exposure

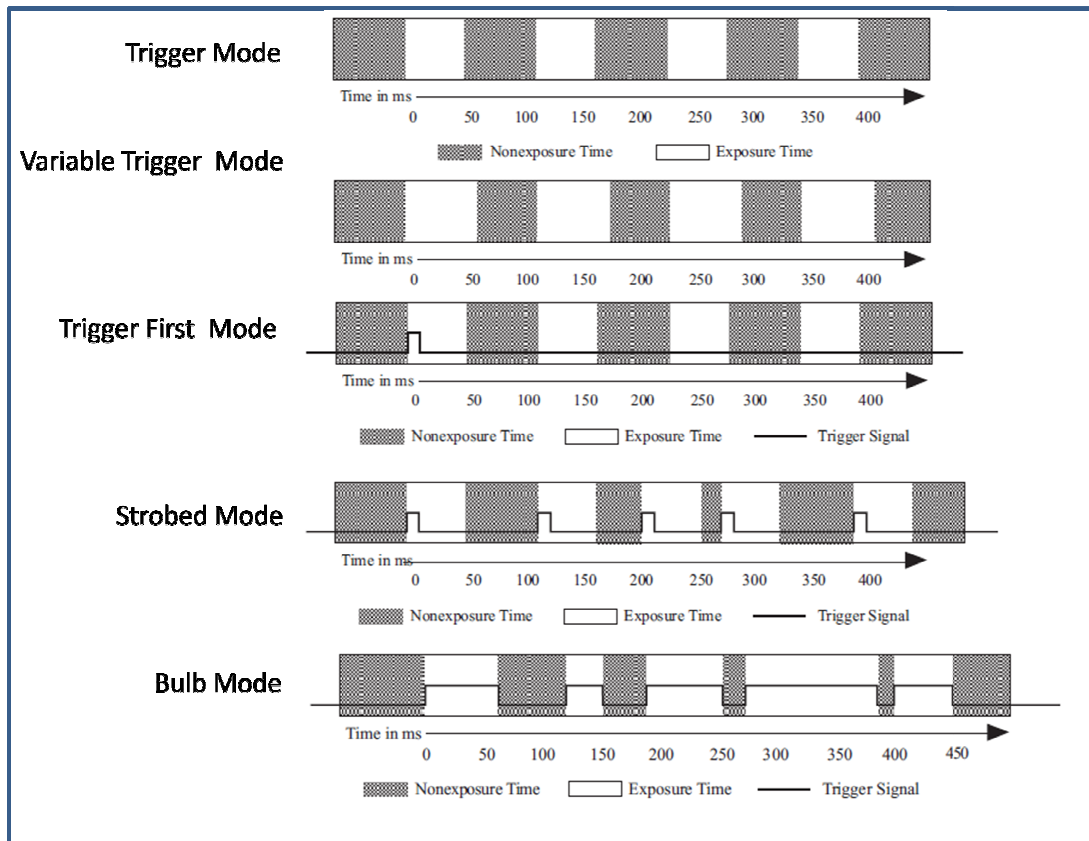


Figure 2.27 Different Exposure Modes © Photometrics

sequence is of constant duration. For the bulb mode, each exposure sequence lasts until duration of each trigger pulse. The figure2.27 shows the schematic working of each of these modes.

The shutter open modes determine how the shutter in the camera behaves when a single exposure is taken or when a sequence is run. Various shutter modes available are PRE EXPOSURE: Opens the shutter before every exposure and then closes the shutter; PRE SEQUENCE: Opens the shutter before the sequence begins and then closes the shutter after the sequence is finished; PRE TRIGGER: Opens the shutter and then clears or exposes (set in clear mode) until a trigger signal starts the exposure; OPEN NEVER: Keeps shutter closed during the exposure, this mode is used for dark exposures; OPEN NO CHANGE: Sends no signals to open or close the shutter. Typically the default shutter mode used is the pre exposure mode.

Clear cycles is another important camera parameter. It is the number of times the CCD must be cleared to completely remove charge from the parallel register. The clear mode is similar to clear cycles; it just indicates the camera when to clean the CCD. Camera gain discussed previously is also a very important parameter as it configures the camera to be responsive to different light-level intensity ranges [photometrics]. The three gain modes discussed previously can be selected from drop down box with Gain3 for High Sensitivity, Gain2 for High Dynamic Range, and Gain1 for High Signal to Noise Ratio. Xanoscope® also continuously monitors the temperature of camera and displays its present and set point value. Xanoscope® is programmed to maintain camera at the optimum temperature of -35°C. This helps to limit the signal to noise ratio and improves efficiency of camera. Further, the spatial and wavelength resolution settings are currently hard coded to 2X2 pixel binning in X-Y direction. Xanoscope® provides a complete automated control over the features of camera, which can be modified as per the specific use of the camera. Xanoscope thus, provides high resolution and high precision image capture.

2.2.1.2 Spectrograph

Spectra Pro 500i spectrograph is driven by Xanoscope® using RS232 serial port interface. Xanoscope® uses application software SpectraPro v3.35 [figure2.28], provided by Acton research to control the spectrograph settings. The basic settings modified in the spectrograph [figure2.28] are its center wavelength and dispersion grating. The current wavelength (center wavelength) at which the grating is positioned determines the range of spectrum wavelengths focused by the spectrograph. Depending on the number of groves on grating, the mechanical scanning range and dispersion properties of monochromator get affected. These two parameters play an important role in calibration of the hyperspectral imaging system discussed later in the chapter. Default parameters currently used are center wavelength of 600nm and dispersion grating of 50 groves per mm, blazed at 600nm.

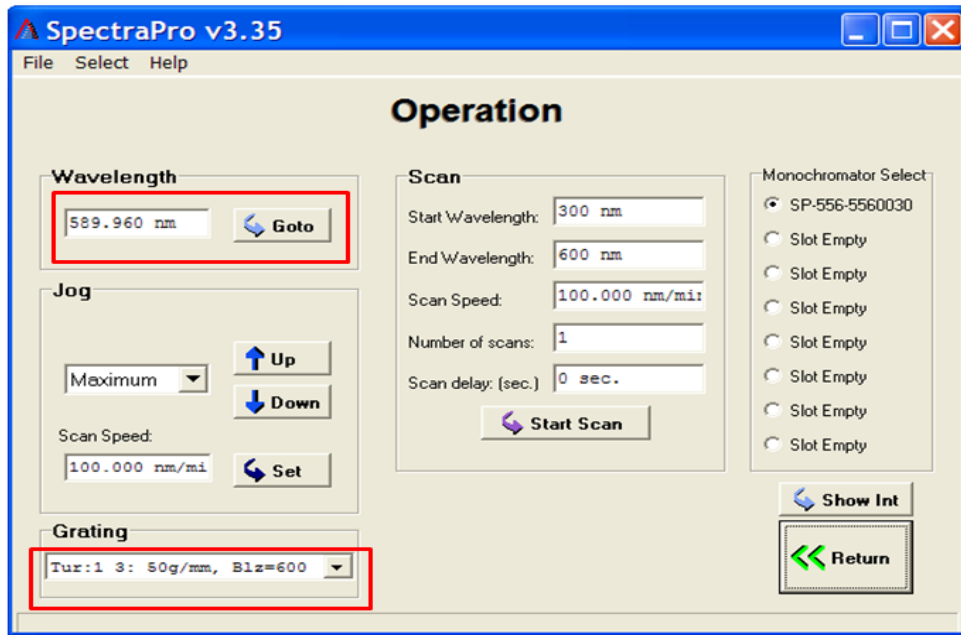


Figure 2.28 SpectraPro ver3.35

2.2.1.3 Stage Motor

The microscope is equipped with a Ludl Electronics Products Ltd. (LEP) micro-mover stage with a MAC 2000 controller interface. This micro-mover stage helps to move the specimen slide across the field of view of the objective lens. The MAC2000 controller provides interface and control of the micro-mover stage. Xanoscope® communicates with this MAC200 controller through a RS232 interface. This interface uses a low level communication protocol i.e. an efficient binary communication protocol for RS232 components [Ludl]. The standard serial

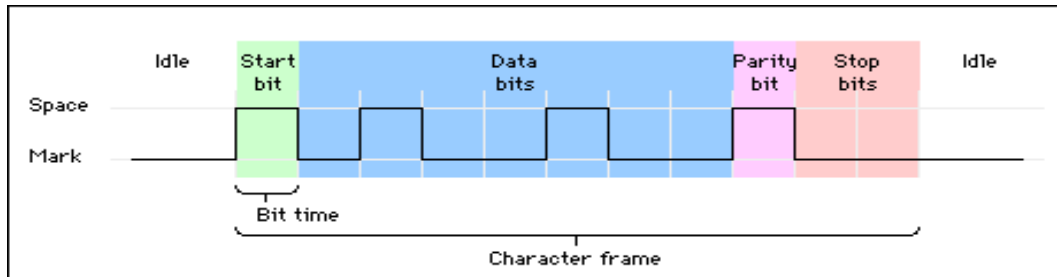


Figure 2.29 Typical Character Frame for RS232 Communication
(Baud Rate, Stop Bit, Data Bits, Parity)
©francis courtis

communication parameters used to interface the stage motor with a computer include the baud rate, data bit, parity and the stop bit [figure2.29]. Baud rate is the measure of how fast data is moving between the instruments that use serial communication. A start bit signals the beginning of each character frame and duration of each character frame. The data bits are used to transfer the commands or data using serial communication. Data bits uses inverted logic i.e. 1 for negative voltage and 0 for positive logic and are read from right to left [11]. In the example below, [table2.4] data bits are interpreted as 1101101 (binary) or 6D (hex) or ASCII letter 'm' [11]. The parity is used for error checking. The logic behind using the parity bit is to indicate beforehand if transmission is odd or even. It also uses inverted logic like the data bits; the figure2.29 above uses odd parity. There are five 1's among the data bits, already an odd number, so the parity bit is set to 0 [11].

Table 2.4 RS232 Interface Settings for Stage Motor

Baud Rate	9600
Data Bits	2
Data Bits	8
Parity	None

Stop bits are the last part of a character frame and consists of 1, 1.5, or 2 stop bits. These bit are always represented by a negative voltage. If no further characters are transmitted, the line stays in the negative else is heralded by a start bit of positive voltage for next incoming character frame. HMI uses the following [table] settings to communicate with LEP stage motor. The minimum step resolution and maximum speed of the micro-mover stage are important controlling parameters to enable fast and efficient data acquisition rates. A LEP micro-mover stage can be driven at a maximum speed of 5 MHz but for safe and optimized operation Xanoscope® is configured to drive stage at about 1MHz (40,000 steps per revolution). The stage moves by only a factor of 0.2µm for every step it takes (minimum step resolution). HMI system uses stage to move the slide across to the next adjacent location. In order to prevent overlapping of these adjacent images it is necessary for the software logic to calculate the exact number of steps required to move to the next position. Xanoscope® calculates the ratio of spatial resolution of single line image to minimum step resolution of the stage (0.2µm). Spatial resolution of image depends on the objective lens and slit width, as discussed earlier in the chapter. It further uses this ratio as the number of steps needed to move stage to the next adjacent position. For example consider a case of a single line image with 0.8µm spatial

resolution then the stage needs to move by a factor of 4 steps in order to move to next adjacent position. This helps to build a stack of individual single line images which are then added together to build the hyperspectral data cube.

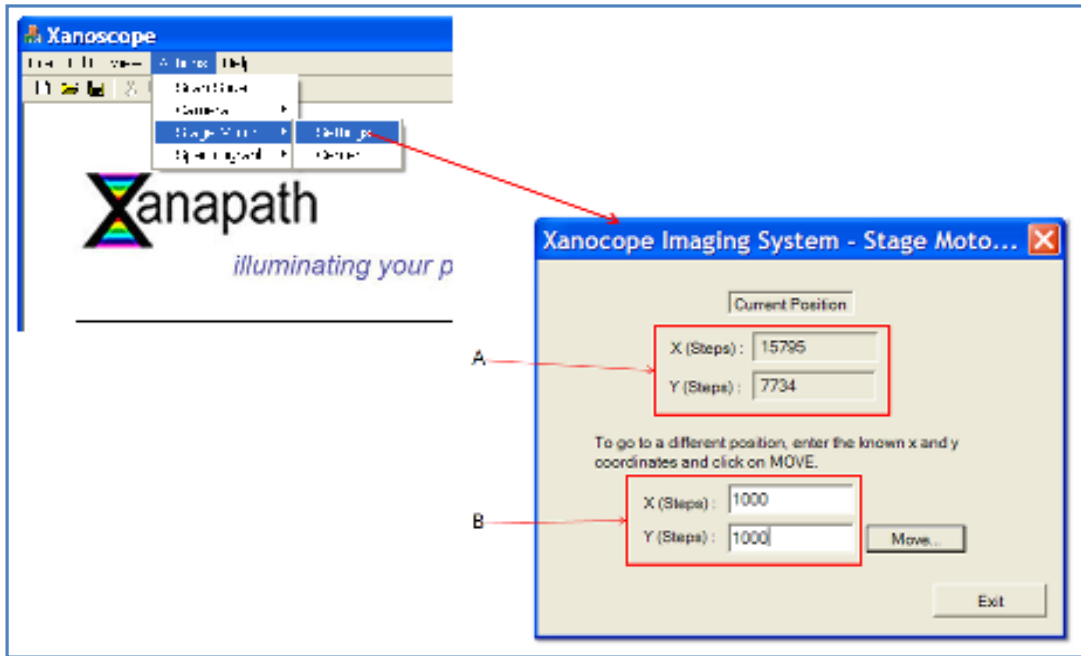


Figure 2.30 Typical Stage Settings Dialog Box in Xanoscope® with (a) Current position of Micro-mover Stage, (b) New Stage Position Co-ordinates

The LEP motorized XY stage consist of X and Y axis motor with limit switches at each end. This limit switches act as mechanical limits to X and Y axis motor. This limit switches are used to center the stage whenever HMI needs to be initialized or calibrated. Xanoscope® achieves this by moving the stage to each of the X and Y limits and record the end point coordinates. It uses these two coordinate positions to find its center coordinates. Once centered, Xanoscope® sets this center position as the origin (0, 0). Xanoscope® can also be used to drive the stage to a known position. Since Xanoscope® records the co-ordinate position for each scan procedure one can revisit this region of interest in the near future by simply entering the known

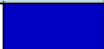









co-ordinate positions [figure2.30]. This also helps to calculate spatial resolution of the region of interest. The figure below shows the typical dialog box for stage settings in Xanoscope®. Here, Xanoscope® displays the current position as well as allow user to enter a new stage position.

2.2.2 Experimental Protocol

The slides were prepared by Dr. Uhr's lab using a standard procedure. For cell lines, about 10,000 cells in 100 µl PBS are placed on each poly-lysine-coated slide. For touch preps, a freshly cut surface of the tumor tissue is gently but firmly pressed onto a slide. All slides are fixed in acetone and stained using a standard immunofluorescence protocol with a mixture of nine antibody-fluorophore conjugates. The concentration for each of them has been carefully chosen by titration. After washing, DNA in the nucleus is stained with mounting media containing DAPI (the 10th color) [Uhr lab]. These slides were scanned on HMI system using a standard mercury arc lamp illumination source, objective lens of 60X Planapochromat Oil and a U-MWU filter cube. The absorption and emission wavelengths of each of the fluorophores are shown in table below.

The fluorophores absorb light from mercury arc lamp source, between ~290nm to ~380nm and then emit light between 411nm~ to 778nm for each pixel. This emission spectrum is captured and used for further quantitative analysis of these fluorophores. The relative contribution of each these marker fluorophore conjugates are computed by deconvoluting the recorded emission spectra. The deconvolution procedure uses standard spectra of each of these fluorophores and the dynamic background spectrum.

Table 2.5 Absorption and Emission Wavelengths of Each of the 10 fluors along with its conjugated antibody and false color used to display each fluor

		Fluorophore	Absorption (nm)	Emission (nm)	Marker
1		AF350	346	442	ER
2		AF488	495	519	Cytokeratin
3		AF532	532	553	Notch-1
4		AF546	556	573	CD45
5		AF568	578	603	PR
6		AF594	590	617	Her-2
7		AF633	632	647	Bcl-2
8		AF647	650	665	Ki67
9		AF660	663	690	GA73.3
10		DAPI	360	461	Nucleus

2.2.3 Data Acquisition using Xanoscope®

Xanoscope® is a comprehensive and user friendly interface that provides the operator an ease when working with microscope. A detailed flowchart of Xanoscope® architecture is shown in [figure2.31]. Once the slide stained with the 10 fluorophores is prepared, the Xanoscope is used to initialize HMI system. The slide is mounted onto microscope and user identifies region of interest. This region of interest is centered onto the field of view of microscope as shown in [figure2.33]. The Initialize tab is usually used to calibrate the HMI system or when a new set of experiments need to run. Initialize will center the stage and load HMI system with its default parameters. A list of all default parameters stored on computer is shown in figure. Once the HMI system is initialized, Xanoscope pops up a scan settings dialog box displaying information relevant for scan procedure to complete.

A typical scan settings dialog box is shown in [figure2.32]. The folder name and location are used to store the raw data captured using HMI system. User can click on the Camera, Stage or Spectrograph buttons in instrument settings group box to view the current status of its device parameters and modify them as per requirements as discussed in section 2.2.1. User needs to check the Standard mode in order to input the number to images and accumulations. The Time Dependent Study mode is used when a fixed location on slide needs to be observed over a period of time. Depending on the size of the area of interest under the microscope, choose the number of images to be taken. Number of accumulations is used to acquire multiple images at same location before moving stage to the next adjacent position.

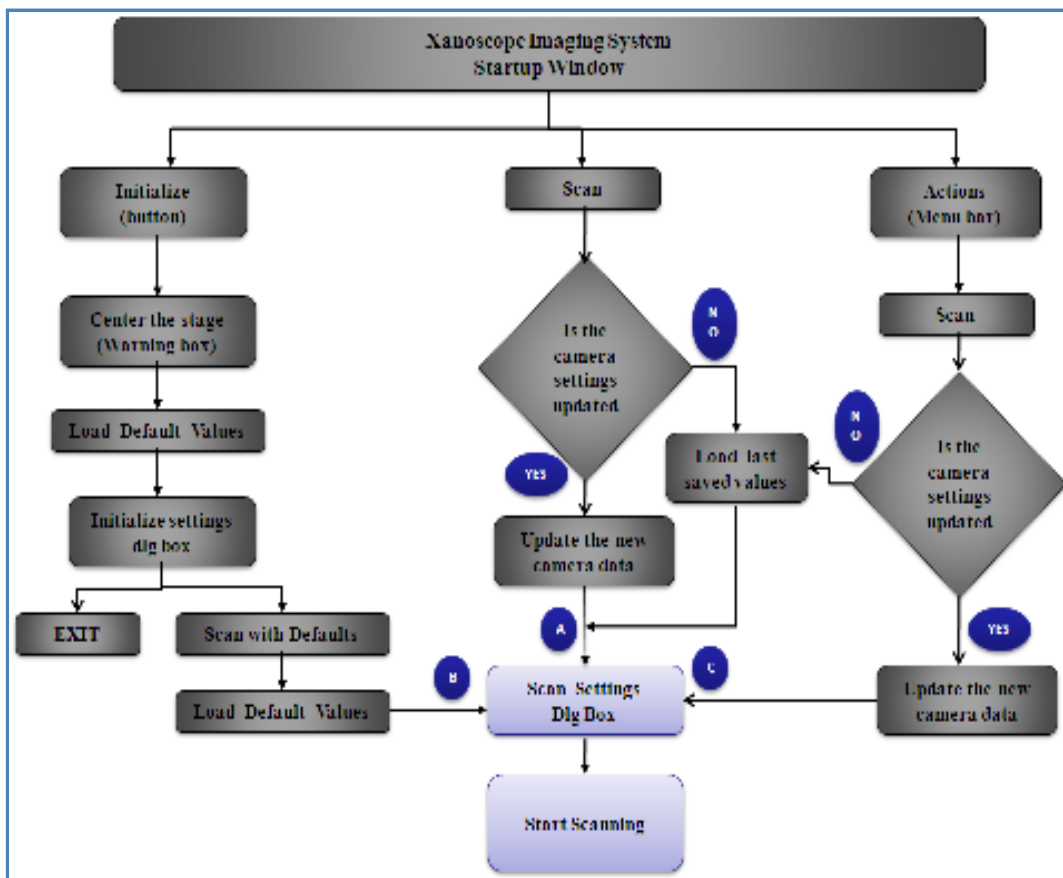


Figure 2.31 A Detailed Flowchart of Xanoscope's Data Acquisition Process in HMI System

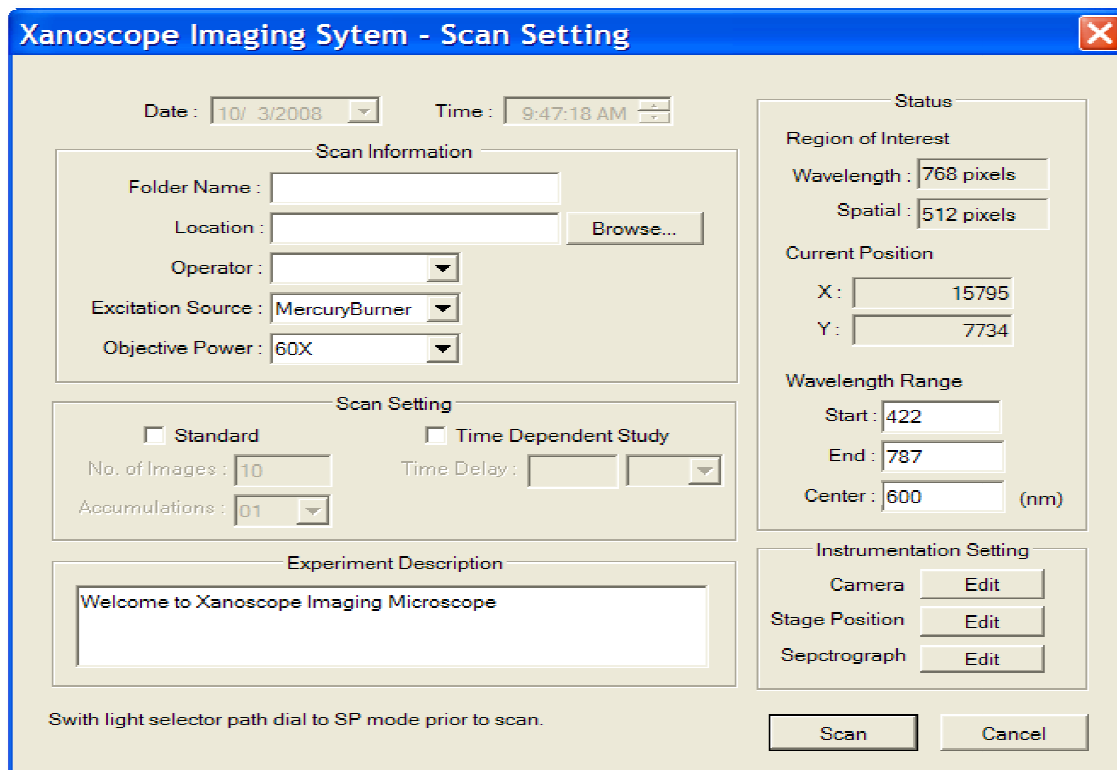


Figure 2.32 A Typical Scan Settings Dialog Box in Xanoscope® to Input Relevant Information for Scan Procedure

Xanoscope adds these accumulated images together and stores it as one single file for that particular position. For example, consider a case with 20 image acquisitions and 3 accumulations. For each acquisition position, Xanoscope will capture 3 images and add them together and store it as one acquisition. Xanoscope follows this procedure for all the 20 acquisitions and stores each of them in the given folder location. This accumulation process helps increase the signal to noise ratio and boost the measured intensity values. Once the parameters in settings dialog box are modified and reviewed, Xanoscope starts scanning procedure. Xanoscope then captures one sample image and gives the scan information in a separate message window. This message window displays the maximum and the minimum count in the spectrum image. When the maximum count value exceeds 4096, saturation takes

place in the image. Saturation indicates that the CCD detector is exposed to long and the charge accumulated in each pixel has reached its maximum. This can be overcome by reducing the exposure time of CCD camera. Also if maximum count is too low it indicates that CCD needs to be exposed for a longer time to accumulate enough charges. The message window also displays the current values of other device parameters along with the total expected acquisition time. It should be noted that the scan information is only from the center of field of view and not the entire scan area. Since the user positions the region of interest in the center of the field of view of the microscope it receives maximum light intensity. Scan information from this center position acts as a reference for the entire image. The user depending on the scan information can either continue scanning or change the values as required before continuing to scan. Since the region of interest is centered to field of view, the stage moves forward to next adjacent position, only right side of the image in the field of view will be scanned. In order to counter this, Xanoscope divides the number of images in half and then moves backwards by that many steps. It then starts scanning from this position in order to cover the full region of interest. For example consider a sample slide as shown in figure 2.34 below. The two cells are focused onto center of field of view of microscope. Consider the user selects 2X2 pixel binning with 60X objective lens, 72 μ m entrance slit width of the spectrograph and 50 images to cover the spatial region that includes the two cells. Xanoscope first calculates the spatial dimension of each single Y- λ image as discussed in section 2.1. Thus each single line Y- λ image is 1.2 μ m in width. Minimum step resolution is 0.2 μ m. Hence to move the stage to next adjacent position Xanoscope moves stage by 6 steps. This helps to prevent the overlapping of images. Now, in order to start scanning the entire region of interest, Xanoscope first moves the stage backwards by a factor of $25 \times 6 = 150$ steps. Xanoscope calculates this by multiplying half of the total number of acquisition i.e. 25 by number of steps needed to move the stage to the next adjacent image i.e. 6. This process is needed to move the stage from the center of field of view to the starting position. Once the target slide is

positioned, Xanoscope starts scanning procedure by capturing a single $Y-\lambda$ image and recording it onto a CCD camera. It then moves the stage forward in X direction to the next adjacent position by moving stage by a factor of six steps, as disused earlier, avoiding overlapping of the adjacent images. This way Xanoscope uniquely acquires 3 dimensional data and stores it onto the user defined location. After Xanoscope acquires all the 50 acquisitions it builds the hyperspectral data cube by adding all the $Y-\lambda$ images together. It then displays this resultant X-Y composite image [figure2.35] on the computer screen along with a separate window [figure2.35] showing all the relevant parameters with which the scan was performed. Along with these relevant parameters Xanoscope also calculates the maximum, minimum and the average count values in the entire composite image, the true spatial X & Y dimension covered in microns and the number of saturated images if any. The resultant X-Y composite image acts as a quick reference for the user to cross check if the scan was ok or not.

Further, Xanoscope provides quick analysis to view the spectrum at any pixel in the composite image. User can browse through the Xanoscope main window to view the display options. First,

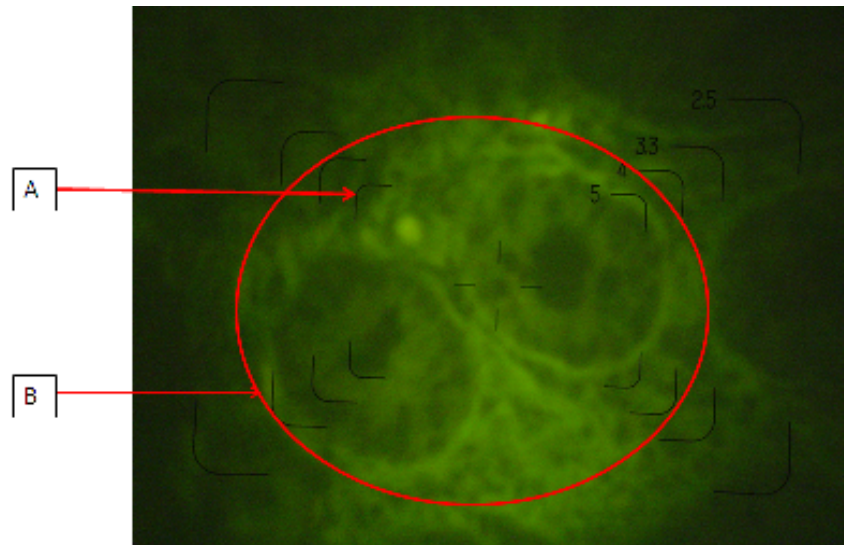


Figure 2.33 A Sample slide with cells focused at the center of field of view of microscope
A: Center Field of View of Microscope
B: Region of interest covering both the cells

is a *Point Spectrum* Figure 2.36 (A), Xanoscope provides the spectrum at the point selected in the composite image. This is very useful as a quick reference to check the spectrum at a particular point of interest in the composite image. Second, is *Row Spectrum* Figure 2.36 (B), Xanoscope provides the spectrum for the entire row associated with the selected pixel in composite image. This feature is particularly useful to view the spectral signature over a entire row of a single cell or target image. This feature also helps to measure the uniformity of CCD array along any pixel row. Xanoscope thus provides automated control over the entire HMI system as well as provides a quick analysis of the resultant hyperspectral data cube.

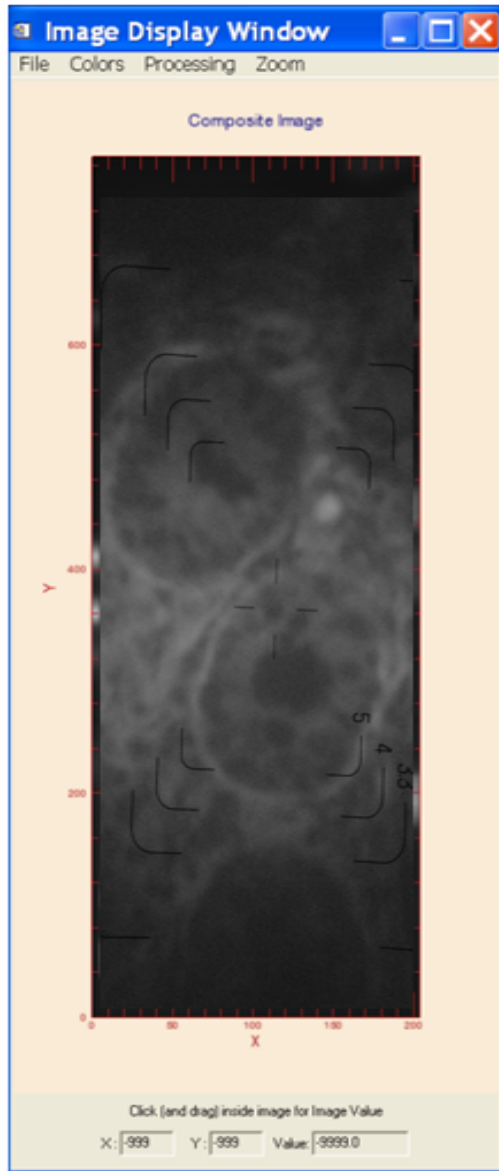


Figure 2.34 A Typical Resultant X-Y Composite Grayscale Image

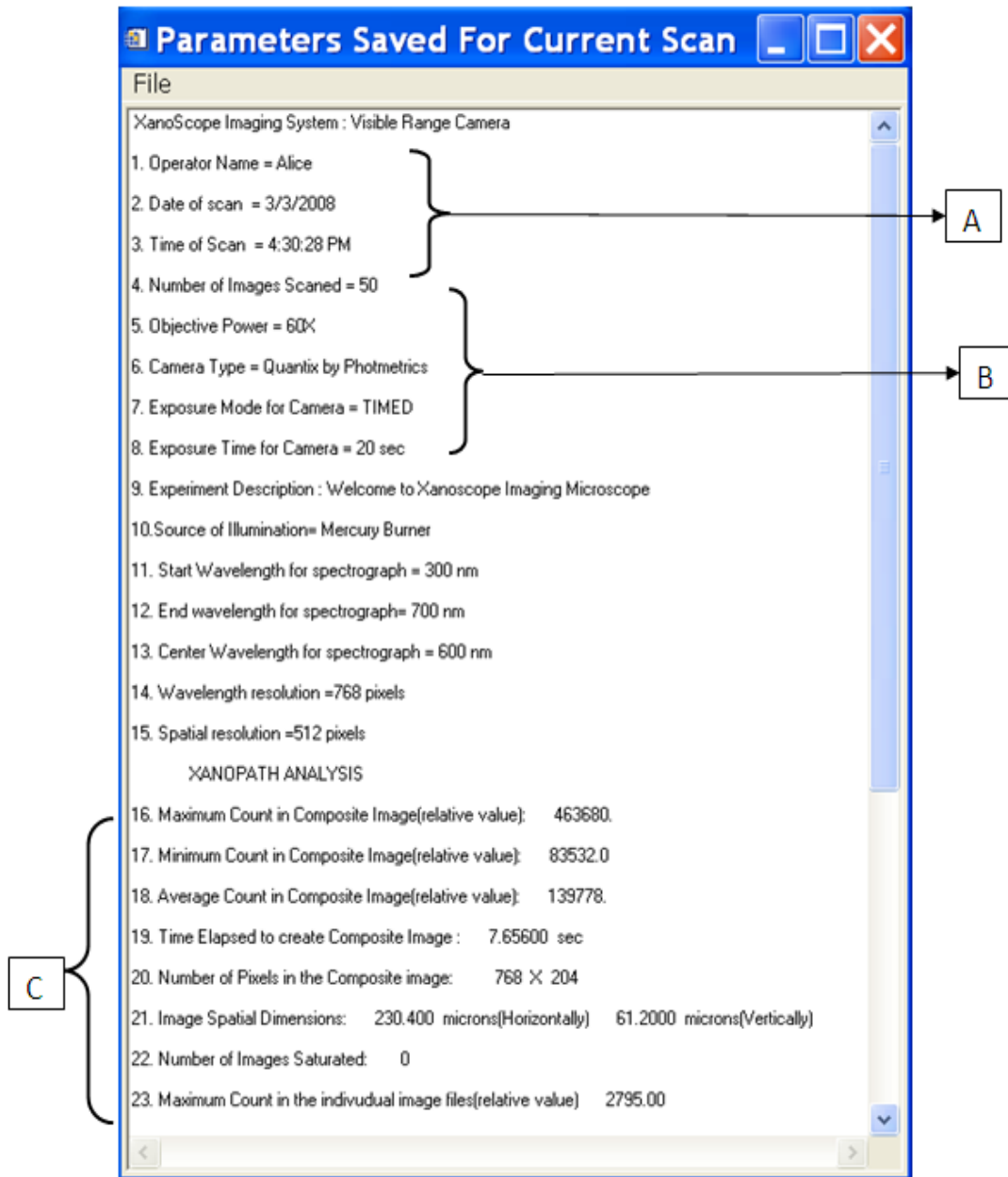


Figure 2.35 A Typical Scan Information Window Displayed along Resultant X-Y Composite Image A: Scan Information, B: Parameters Information, C: Analysis Information including Spatial Dimensions and Intensity counts from the composite image

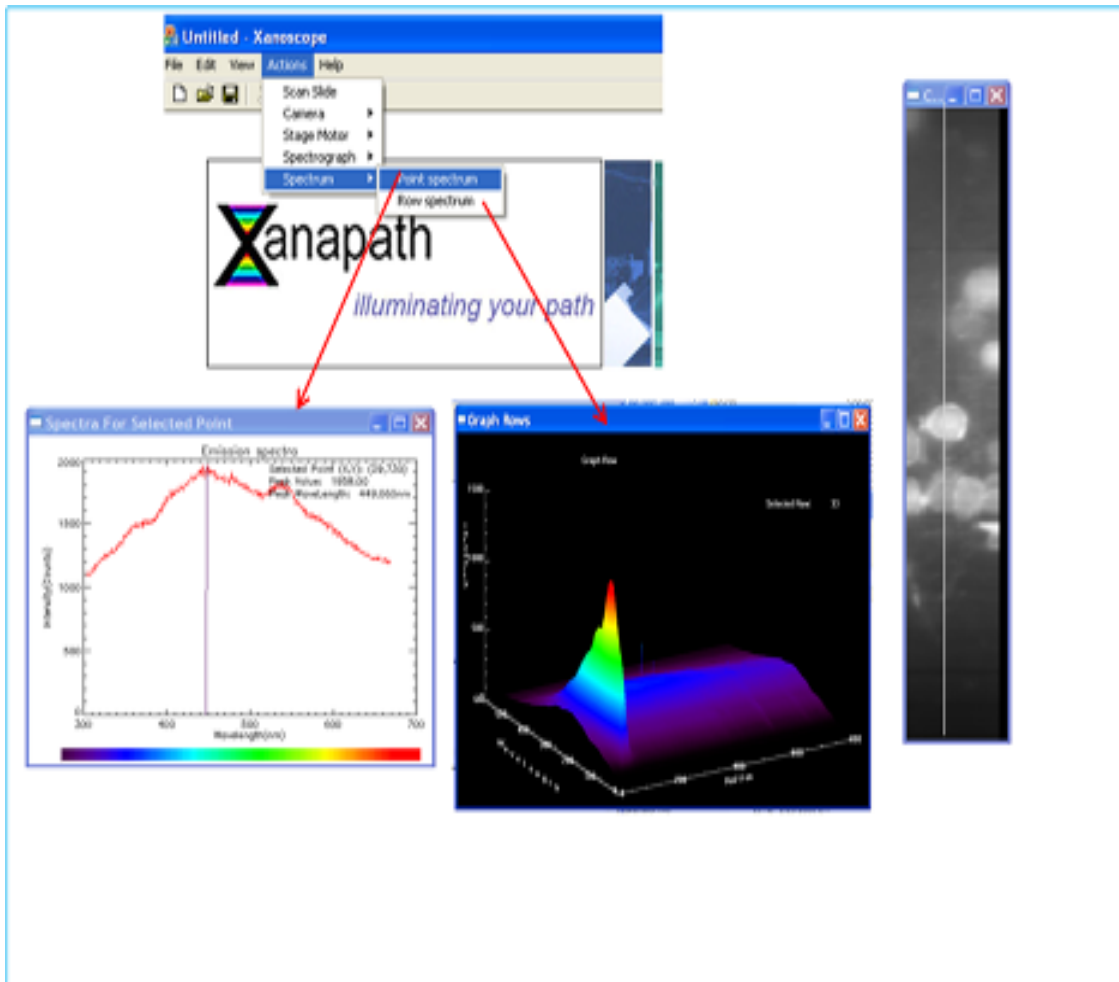


Figure 2.36 Quick Review of Spectrum in Hyperspectral Data Cube using (a) Point Spectrum- It gives spectrum at any given pixel in image by clicking at any point in image and (b) Row Spectrum—It gives spectrum along the entire row of selected pixel in an image

CHAPTER 3

RESULTS AND DISCUSSION

The overall goal of this chapter is to discuss the validation of the system specifications. The chapter is divided into two basic sections. Section one deals with the validation of the system parameters, which are used in Xanoscope®. The second section deals with results obtained from analyzing the data acquired using the software. The data is acquired from tissues stained with 10 different fluorophores.

3.1 Software Validation

3.1.1 Determination of Spatial Resolution

The spatial resolution of the hyperspectral image acquired depends on the CCD camera pixel size and microscope magnification. As discussed in section 2.1.4, the Quantix camera has a CCD array of 1536X1024 pixels with a pixel pitch of 9X9 μ m. Xanoscope bins the CCD camera at 2pixels in both directions making the size of each image 768x512 pixels. It aligns 768 pixels in spatial direction (Y-direction) to allow the greatest spatial acquisition per exposure. The imaging spectrograph also contributes to the spatial resolution of the hyperspectral image. The width of the narrow entrance slit of the spectrograph determines the width of light focused onto the dispersion grating. Thus, the Y-axis is aligned along the height of the slit and X axis along the width of slit. The slit of spectrograph is positioned at 72 μ m based on the relative intensity response to the spectrograph slit width as discussed in Chapter 2 section 2.1.2. Xanoscope acquires individual pictures along the Y- λ plane, while the stage is incremented in the X-direction to cover the entire region of interest. Xanoscope thus builds a resultant X-Y image

from collection of such 3 dimensional images. While on the other hand, the X direction spatial resolution, is determined by the slit width of the spectrograph and microscope magnification. As discussed before, let the X and Y dimensions of the CCD pixel be δx and δy respectively and the magnification be M. Let W_s be the slit width of the spectrometer. The spatial resolution in the Y direction is $2\delta y/M$ and the spatial resolution in the X direction is W_s/M . In normal operations, Xanoscope is initialized with binning of 2 pixels in both X and Y directions and the entrance slit width is $72\mu\text{m}$. Thus, the spatial resolution of the resultant X-Y image is $(2 \times 9/60) = 0.3\mu\text{m}$ per binned pixel in Y direction and $(72/60) = 1.2\mu\text{m}$ in X direction. Thus, a single image captured using Xanoscope® has spatial resolution of $0.3\mu\text{m}$ by $1.2\mu\text{m}$ per image pixel in Y and X direction respectively.

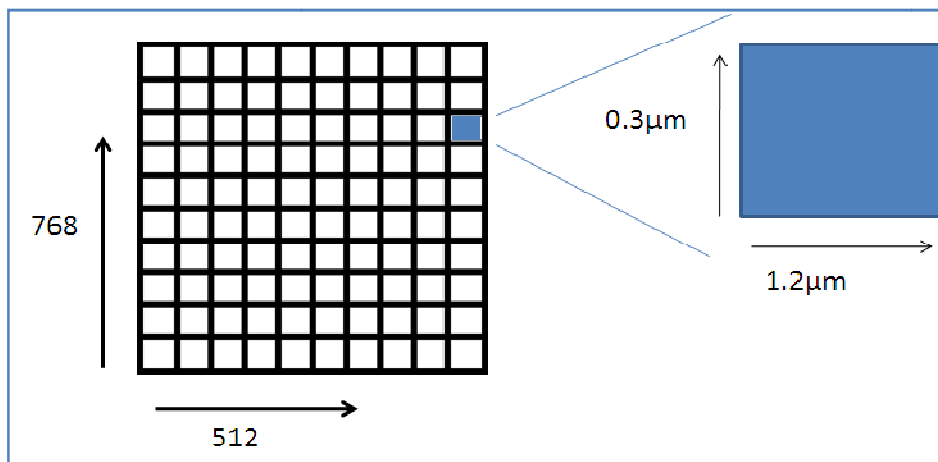


Figure 3.1 Figure shows spatial resolution of a pixel for a 2x2 binned image at 60X objective and $72\mu\text{m}$ slit width and 768x512 pixels

3.1.2 Determination of the Field of View

The total field of view of the image acquired using Xanoscope depends on the number of pixel columns in CCD array and the microscope magnification. In normal operations, Quantix CCD array is binned by a factor 2 pixel in both X&Y direction. Then the field of view is $768 \times 9 \times 2/60 = 230.4\mu\text{m}$ in Y direction and $72/60 = 1.2\mu\text{m}$ in X direction. Thus, each single image captured using Xanoscope® has $115 \times 78\mu\text{m}$ field of view in Y and X direction respectively

3.1.3 Validating the Linearity of CCD Camera through Xanoscope

Linearity is a measure of how consistently the CCD responds to incident light. The transfer function of the system is given by the incident photonic signal and the final digitized output. The transfer function should ideally, vary linearly with the amount of light incident on the CCD. In order to see this linearity, average intensity counts in each image is plotted vs Xanoscope controlled exposure times. From the figure, it is observed that the average intensity counts in each image vary linearly with increase in exposure time. These data points were then fitted with linear regression analysis. The R^2 value of 0.98 was observed. This validates linearity of CCD camera through data acquired using Xanoscope. It also proves that the intensity counts read by Xanoscope are real and allow quantitative measurements of the image. This can be used in quantifying the expression levels of multiplexed fluorophores.

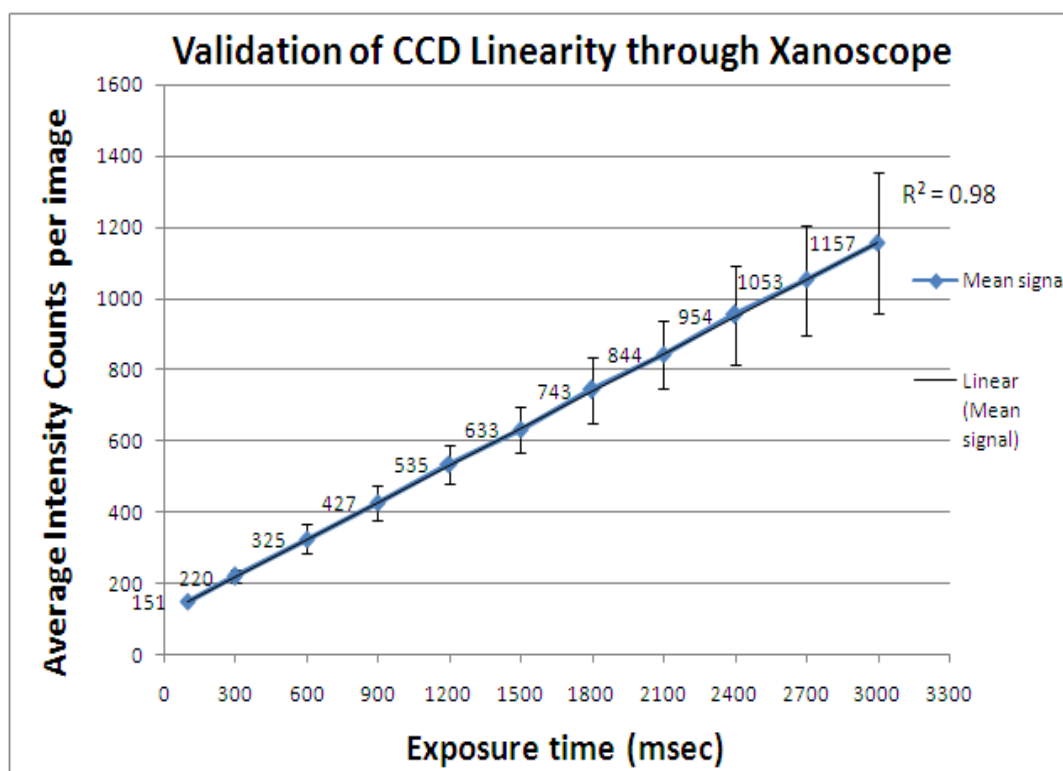


Figure 3.2 Figure shows the validation of CCD linearity using data acquired by Xanoscope. For these images were obtained at different exposure time with all other parameters being same. A linear regression analysis performed over these values indicate R^2 value of 0.98 validating the linearity of CD camera controlled by Xanoscope

3.1.4 Validating Gain Settings of the Camera

The gain of Quantix 1602E CCD camera determines how the amount of charge collected in each pixel of image will be assigned to a digital number in the output image, as discussed in section 2.1.4. For gain2, the full well of its CCD matches the full range of digitizer at a relative gain 1x. Similarly, for gain1 (1/2x) and gain3 (4x), its full well matches the full range of digitizer. Thus the total signal accumulated (gray levels) on ADC in gain1 is half of gain2 and gain3 is 4 times of gain2. Xanoscope captured three images with same parameter settings except for different gains settings for each image i.e. gain1 (high signal to noise mode), gain2 (high dynamic range mode), gain3 (high sensitivity mode). Xanoscope calculates the average intensity counts (gray levels) in each of these three images. These average intensity counts



Figure 3.3 Figure shows the average intensity counts (gray levels) in each image at 3 different gain settings, gain1 is high signal to noise ratio mode with relative gain of $\sim 1/2 X$, gain2 is high dynamic range mode with relative gain of $\sim 1X$ and gain3 is high sensitivity mode with relative gain of $\sim 4 X$. Accordingly the average intensity counts vary by a factor of $1/2 X$ for gain1, $1 X$ for gain 2 and $4 X$ for gain3

(gray levels) are plotted against gain settings as shown in figure 3.3 below. Average intensity of the image for gain1 is 347, for gain2 is 644 and gain3 is 2275. This validates that the average intensity counts (gray levels) in the image acquired using Xanoscope varies by a factor of relative gain of its gain setting. Since for gain1 (1/2x) the average intensity count in image is approximately half of that of gain2 (1x) and the average of intensity count in the image for gain3 (4X) is approximately four times that of gain2 (1X).

3.1.5 Validation of Accumulations Functionality of Xanoscope

For low light imaging, every single photon counts. Thus it is necessary to ensure that the signal level relative to noise is adequate to allow capture of accurate image information. To overcome this, Xanoscope provides an accumulations functionality as discussed in sections 2.2.3. Depending on the number of accumulations, Xanoscope captures multiple exposures at the same location before moving to the next adjacent position. It then adds these multiple exposures of the same image and saves it as one single image. Accumulations work on the assumption that the noise in the image is truly random, which is true for most cases. Accumulations thus remove any random noise in the image and also increase the total number of counts in the final image without compromising any detail. Accumulations may also increase the bit depth of the image beyond what would be possible with just a single image. Accumulations can thus be especially useful to increase the sharpness of the image. This way, random fluctuations above and below the actual image data will gradually even out as one accumulates more images. Figure 3.5 and 3.6 below shows that, the average intensity counts over the composite image vary linearly with the number of accumulations in each scan. All scans were carried out at 60 X objective power, high sensitivity mode of gain 3; spectrograph slit width of 72 μ m and total of 30 images for each experiment. Thus the only varying parameter was the number of accumulations. It can be observed from the figure below, that as the number of accumulations increases the image contrast and sharpness improves.

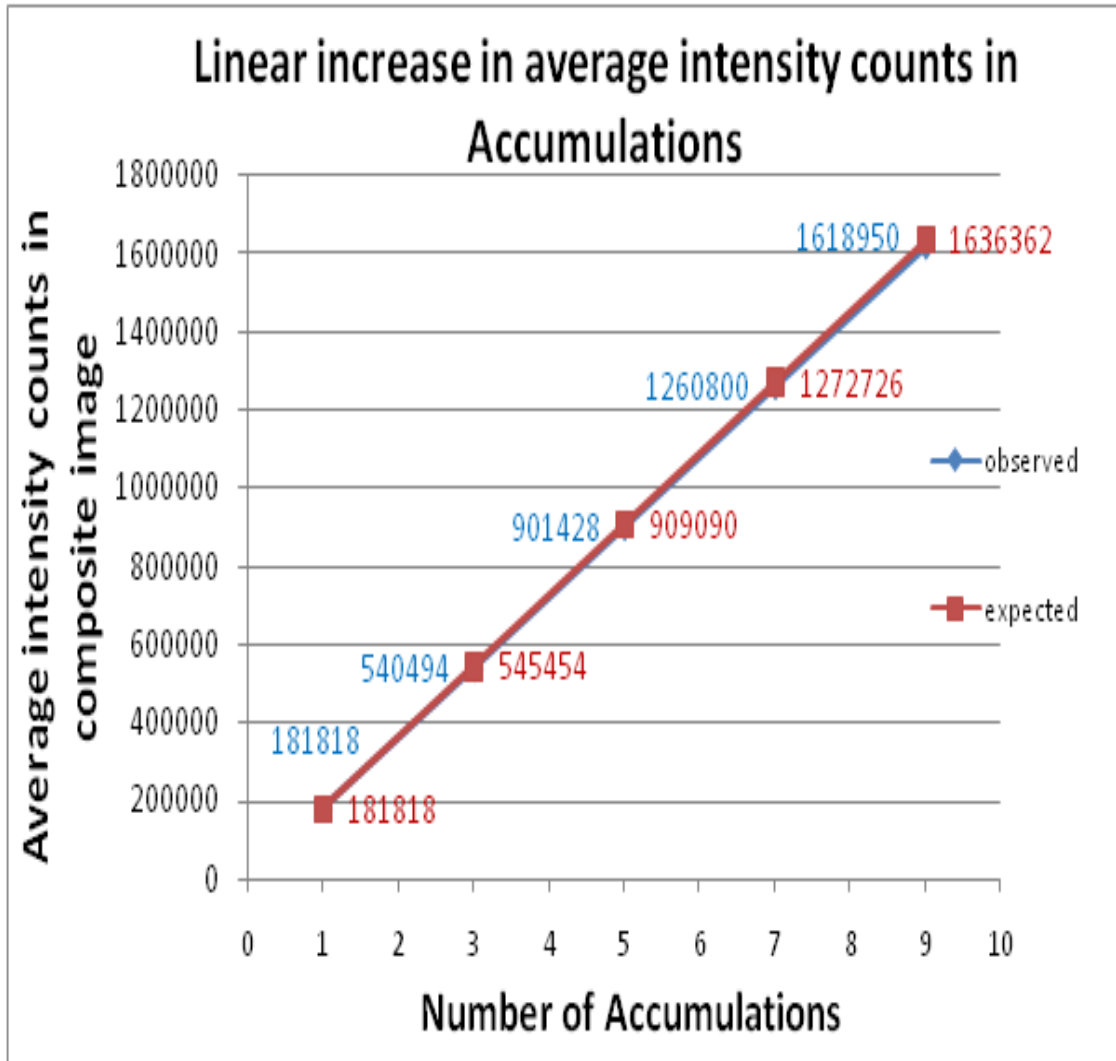


Figure 3.4 Figure shows linear increase in average counts in composite image with linear increase in number of accumulations i.e. 1,3,5,7 and 9 thus validating the accumulations functionality. All the images were captured at 60X objective power; 72 μ m spectrograph slit width, exposure time of 3 seconds, 30 acquisitions and Mercury arc lamp source for each experiment

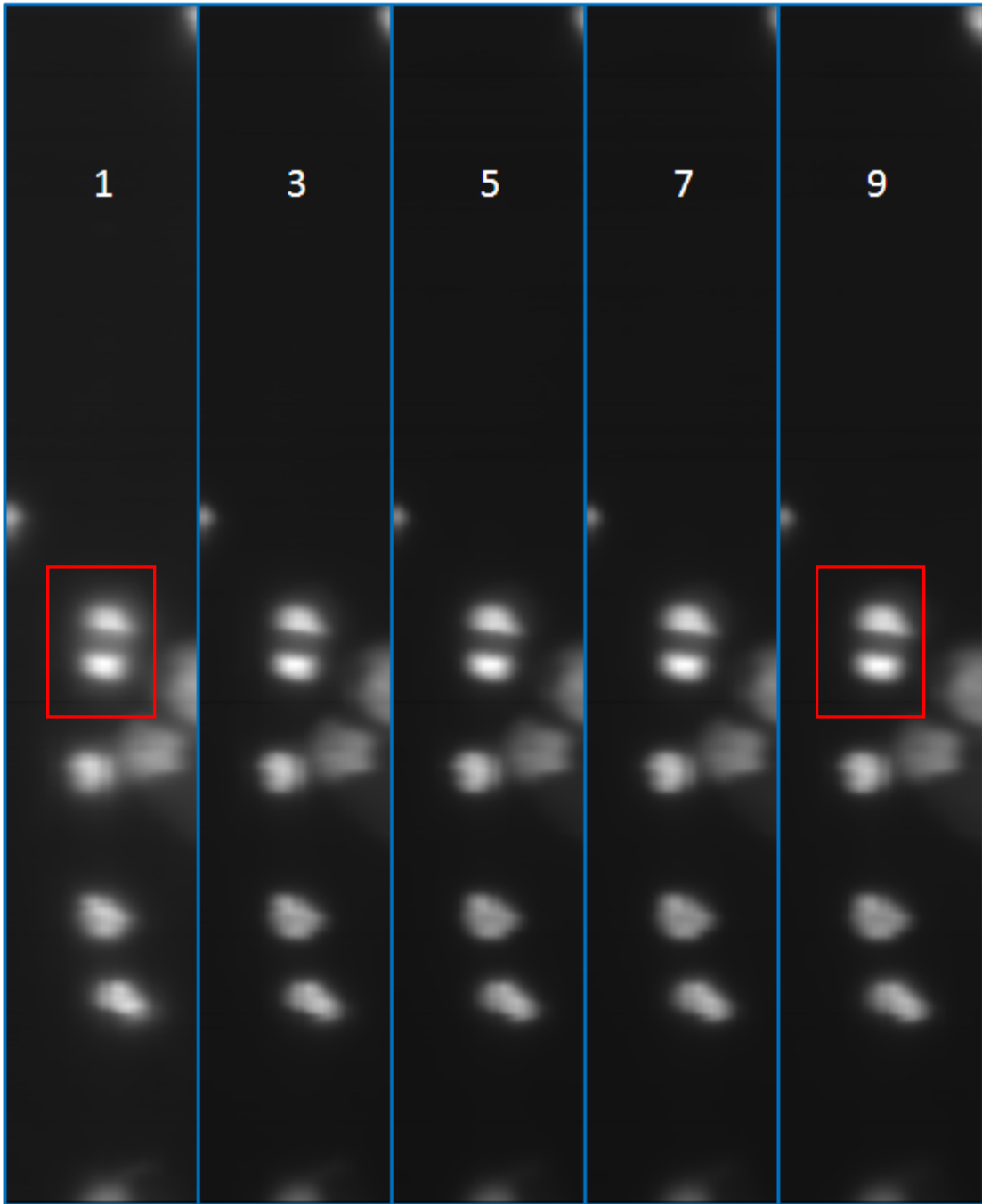


Figure 3.5 Figure shows composite images acquired 1,3,5,7 and 9 accumulations each. It shows the improving contrast and sharpness of the image from 1 accumulation to 9 accumulations, validating that accumulations help improve signal to noise ratio. Each composite image was built at 60X objective power, 3 seconds exposure time; 72 μ m spectrograph slit width and 30 acquisitions.

3.1.6 Validating Xanoscope's Accurate and Precise Control over the Movement of Stage

The micro-mover stage is an important component in the hyperspectral imaging system, as it required to move the slide over the optical path of microscope. To build up the hyperspectral data cube the micro-mover stage needs to move the sample slide across precisely by the number of steps required to move to next adjacent position. It is designed to avoid overlapping of adjacent images and also prevents skipping areas between adjacent images. The figure below shows validation of such precise movement of stage using Xanoscope. A calibration slide marked with a scale of $10\mu\text{m}$ for each division was used to indicate precise control of stage by Xanoscope.

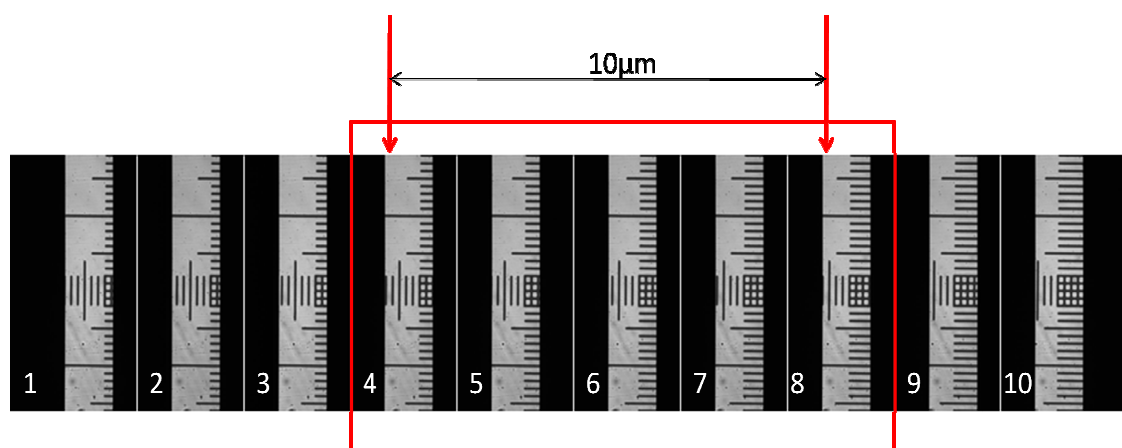


Figure 3.6 Figure shows the precise control of Xanoscope over micro-mover stage. 10 images were captured at 100msec and 40X magnification and slit width of $80\mu\text{m}$ and each division on scale is $10\mu\text{m}$. For image 4 to 9 the stage has moved by $10\mu\text{m}$ and from divisions on scale too its $10\mu\text{m}$ this validates Xanoscope's precise control over stage.

Xanoscope acquires 10 images with 40X magnification and $80\mu\text{m}$ slit width at 100msec exposure time. Since the minimum step size of the stage is $0.2\mu\text{m}$ and from the magnification and slit width, each image is a view of the calibration slide as seen from $80/40=2\mu\text{m}$ to the right of the previous image. The total number of steps needed to move over each image is $2/0.2=10$ steps. Now for image 4 to 9 we can observe that stage has moved over 1 division i.e. $10\mu\text{m}$. From Xanoscope calculations it has 5 images with 10 steps in each image i.e. $5*10=50$ steps. With a minimum step size of $0.2\mu\text{m}$, the total spatial position moved by Xanoscope is

50*0.2=10 μ m. This validates that Xanoscope provides accurate and precise control over stage. This also validates that the hyperspectral data cube built using Xanoscope has no overlapping or skipped area over adjacent images. Thus Xanoscope provides full spatial coverage of a scanned sample region.

3.2 Performance Evaluation

In this section, the performance of Xanoscope is evaluated through identifying and measuring the expression levels of multiplexed fluorophores conjugated to tumor markers. Further the section also discusses the statistical results and analysis of these fluorophores.

3.2.1 Characterization of multiplexed fluorophores

As discussed in chapter2, section 2.2.2, various cell lines stained with nine antibody-fluorophore conjugates along with DAPI contained in mounting media were used to evaluate system control with the Xanoscope software. The scans were carried out at 60X magnification, slit width of 72 μ m, and high sensitivity mode (gain3) i.e. 4x. The slide were scanned using the mercury arc lamp with wavelength band filter of ~290nm to ~380nm to excite the fluorophores and capture spectra with emission wavelengths between 411nm~ to 778nm for each pixel. The Figure3.7 below shows standard emission spectra of twelve fluorophores. From this, we use ten fluorophores for our study excluding AF350 and ToPro3. The marker table which lists the antibodies conjugated to these ten fluorophores along with fluorophore absorption and emission spectra is shown in table3.1. As discussed in section 2.2.2, these ten fluorophores are conjugated with antibodies for different cell lines such MCF7 – breast cancer cell line, Skbr3 - breast adenocarcinoma cell lines, Daudi - Human Burkitt's lymphoma cell line and touch preps (TP) from breast cancer patients and also normal breast cells. The relative contribution for each fluorophore at any pixel of an image was calculated using analysis software developed in house by Michael Huebschman. This analysis software uses linear unmixing algorithm to deconvolve the multiplexed fluorophores.

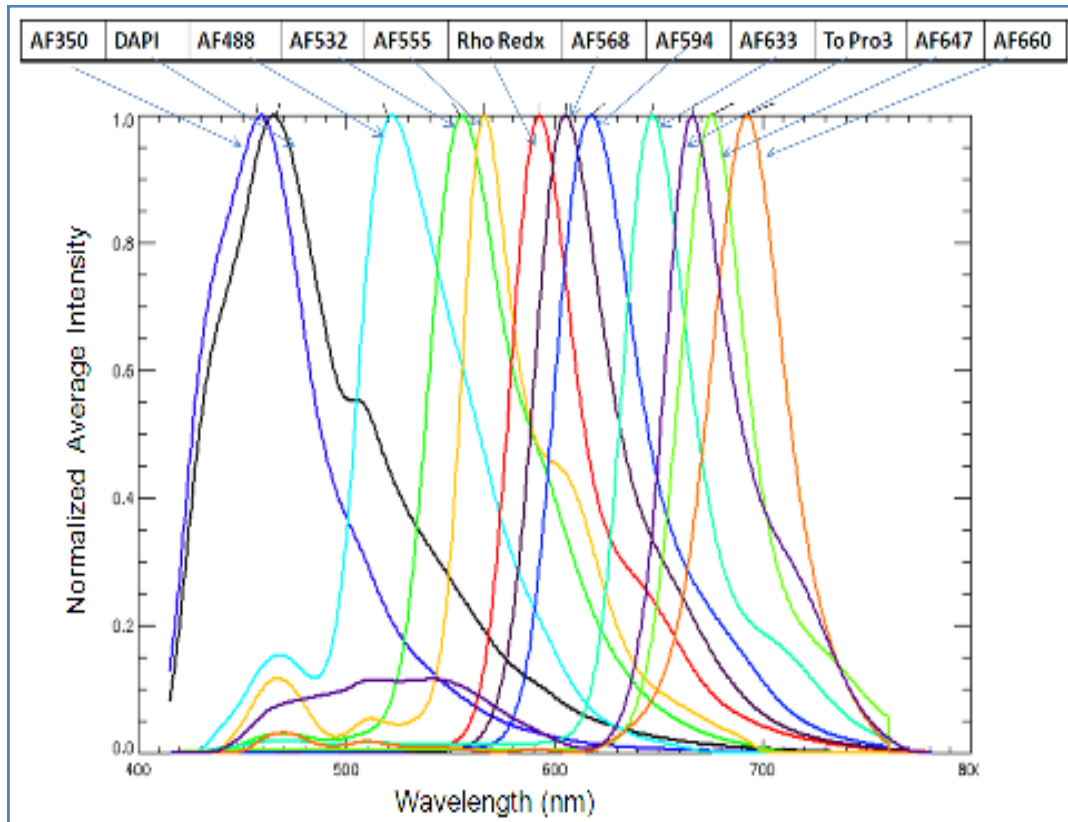


Figure 3.7 Figure shows standard emission spectra of 12 fluorophores acquired using Xanoscope. These are used as reference spectra to deconvolve individual fluorophores and measure their contribution in any pixel in an image

Table 3.1 Figure shows the marker table of the ten fluorophore-antibody conjugates with peak absorption and emission wavelengths of each fluorophores along with localization of its expression in the cell

	Color	Dye	Ab/Ems	Biomarkers	Localization
1	[0, 255, 255]	DAPI	360/461	DNA/Nucleus	nuclear
3	[0, 255, 0]	AF488	495/519	Cytokeratin	cytoplasm
4	[255, 255, 0]	AF532	532/554	Notch-1	cytoplasm
5	[255, 0, 0]	AF555	555/565	CD45	cytoplasm
11	[200, 0, 50]	Rhodamine Red X	570/590	ER	nuclear
6	[200, 55, 0]	AF568	578/603	PR	nuclear
7	[255, 50, 50]	AF594	590/617	Her-2	cytoplasm
8	[255, 0, 110]	AF633	632/647	Bcl-2	cytoplasm
9	[190, 0, 200]	AF647	650/668	Ki67	nuclear
10	[155, 0, 0]	AF660	663/690	EpCAM	cytoplasm

The working of analysis software can be best explained through Figure 3.8 shown below. Consider the reference spectra of two fluorophores R1 and R2. Assume that, the spectra at a given pixel (x,y) in an image $S(x,y)$ is obtained from hyperspectral imaging. Now in order to calculate the individual fluorophore contribution at that particular pixel linear unmixing algorithm is used. We know that the spectrum at the pixel is mixture of R1 and R2 combined together. Thus it some number A_1 times reference spectra R1 and A_2 times second reference spectra R2. Let us assume that, the numbers A_1 and A_2 are linear, then as shown in equation A_1 and A_2 are linear so they add up to 1. Now since we know the spectra at that pixel and also at the reference spectra, we can easily compute the contributing factor A_1 and A_2 by substituting A_2 as $1-A_1$. Similarly linear unmixing model is used to unmix all ten multiplexed antibody-fluorophores conjugate and measure the contribution of each at any pixel of image.

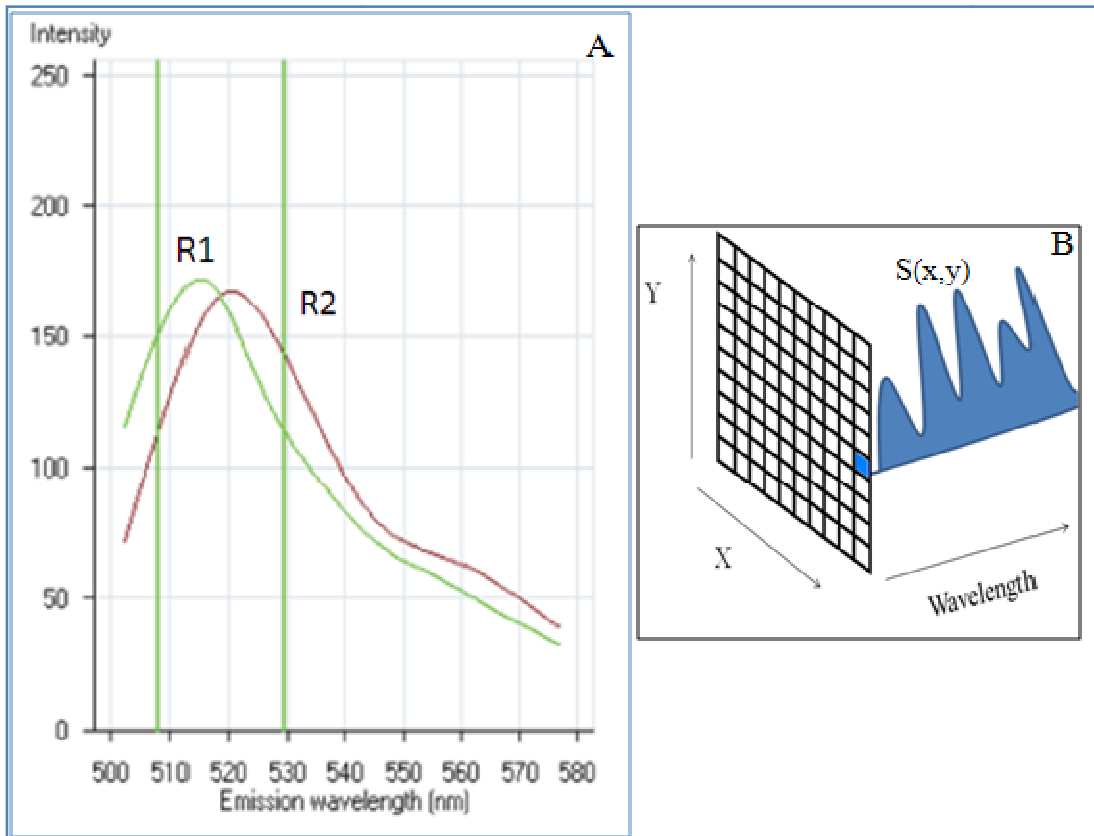


Figure 3.8 (a)Reference spectra for two sample fluorophore R1 and R2 and (b) $S(x,y)$ is spectra at any pixel in an image

$$S(x,y,\lambda) = A1(x,y) \times R1(\lambda) + A2(x,y) \times R2(\lambda) \dots\dots\dots 1$$

$$A1 + A2 = 1 \dots\dots\dots 2$$

Equation. 1 and 2 indicate a typical linear unmixing model

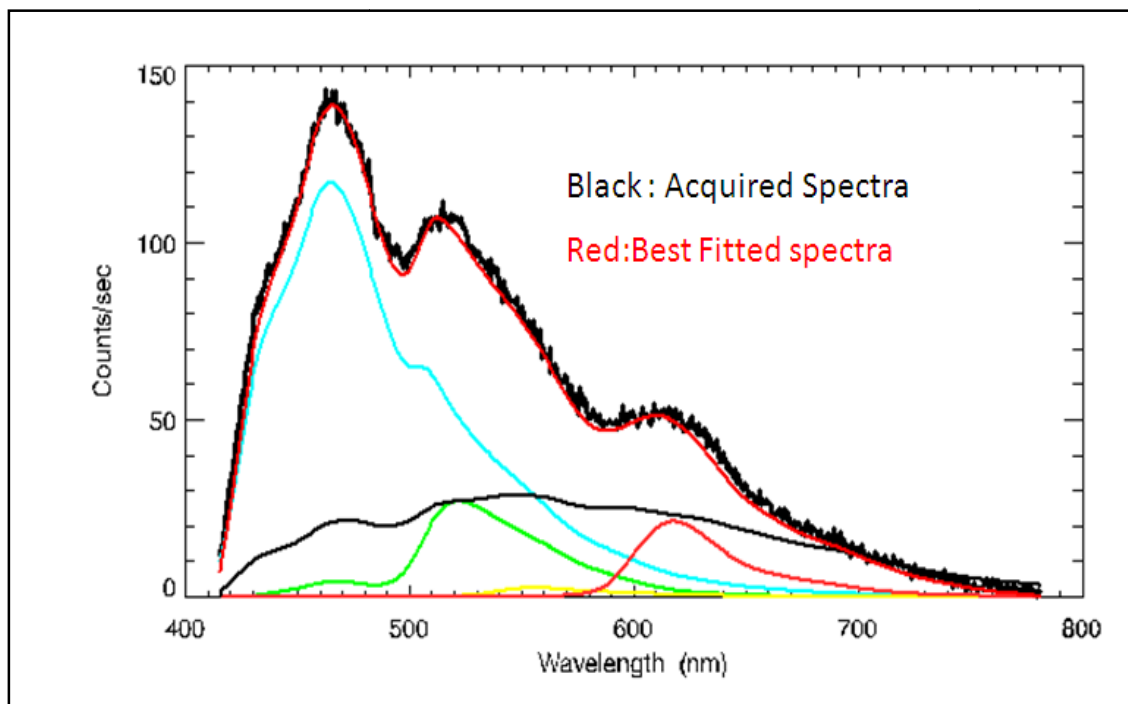


Figure 3.9 Figure shows process of evaluating the contribution each fluorophore algorithmically using a linear unmixing process the red curve is the best fit for acquired black spectra based on reference spectra of each fluorophores (curves shown in the other colors)

Using these unmixing algorithms and reference spectra of fluorophores from [Figure3.7] the spectra at each pixel is compared with the resultant spectra from linearly adding all these individual reference spectra and accepting the best fit least squares fit values as shown in Figure3.9. These values are relative contributions of each of fluorophore at that particular pixel. The contribution of each fluorophore can then be viewed independently and as quantitative cell-

averaged intensities. Morphological measurements (nuclear to cell area, cell circularity) are also output to the user. The Figure 3.10 below shows such quantitative cell averaged intensities of each fluorophore and Figure 3.11 shows the marker table along with the expression levels for the individual cell lines, touch preps and normal cells from literature provided by Uhr lab. From both of these, we can analyze the expression levels of fluorophore- antibody conjugates from data acquired using Xanoscope and compare them with expression levels mentioned in the literature. This proves that Xanoscope provides with sensitive and high resolution data from highly multiplexed fluorophore- antibody conjugates. This can be further analyzed using standard analysis techniques to identify the contribution of individual fluorophores.

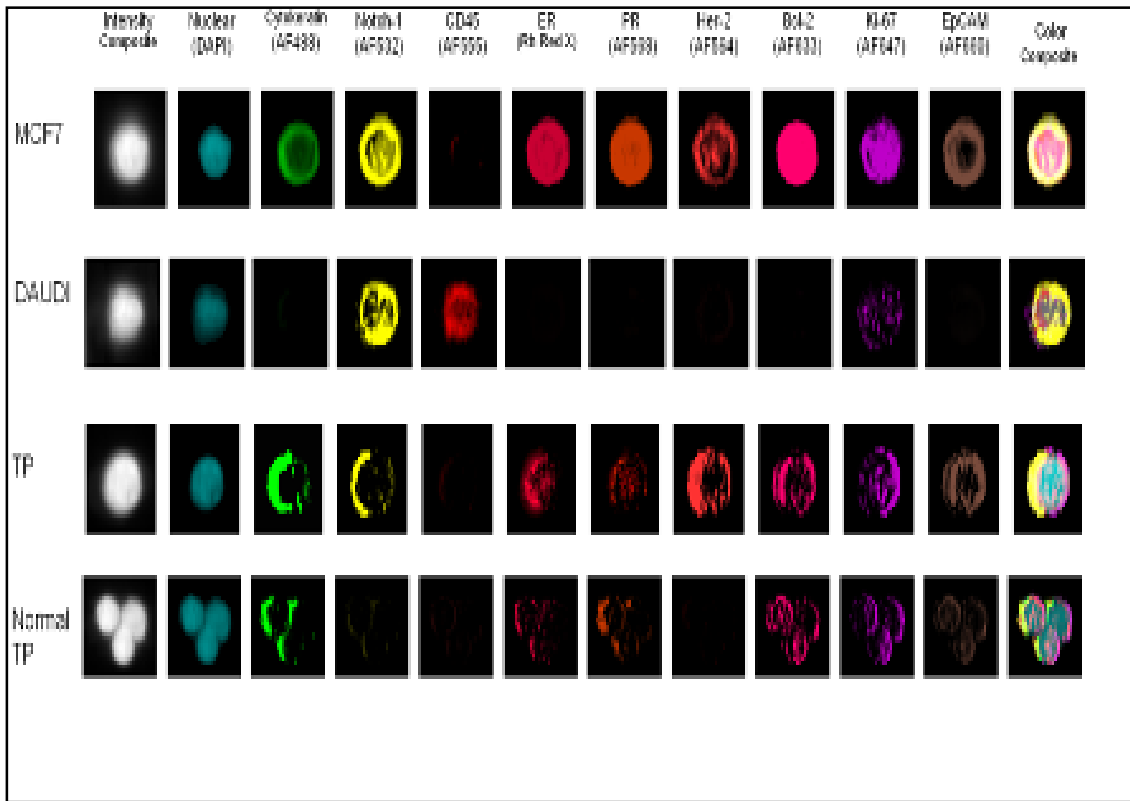


Figure 3.10 Figure shows visualization of individual contribution of fluorophores-antibody conjugates in MCF7- breast cancer cell, Daudi - Human Burkitt's lymphoma cell line and Touch preps from breast cancer patients and also normal breast cells.

3.2.2 Statistical analysis of quantitative data extracted from Multiplexed Fluorophores using Xanoscope

As discussed in the previous section the contribution of each fluorophore-antibody conjugate is calculated by deconvolving the spectra at each pixel from data obtained using Xanoscope. This deconvolution data also provides with the relative intensity counts for each of these multiplexed fluorophores. These intensity counts are used to relate the intensity quantification numbers to the level of expression for statistical analysis. The graph from Figure 3.11 shows the values for average tumor marker intensity (averaged over the area of the cell) in cell lines and TPs. Dividing the average value by the value at 1, standard deviation for the distribution of marker values for cell lines known to be positive and negative enables us to normalize the output. Hence, HMI numbers for 1 and below indicated no over expression.

Table 3.2 Table shows the expression of fluorophore-antibody conjugate for MCF7 and Daudi cell line and also from cells of cancer patient and normal breast cells

No.	Fluorophores	Markers	Expression			
			MCF7	Daudi	Touch Prep	Normal
1	DAPI	Nuclear	+	+	+	+
2	AF488	Cytokeratin	+	-	+	-
3	AF532	Notch-1	+	+	+	+ (NK cells)
4	AF555	CD45	-	+	-	+
5	Rhodamine Red X	ER	+	-	+	May be
6	AF568	PR	+	-	+	no reports
7	AF594	Her-2	+	-	+	-
8	AF633	Bcl-2	+	-	+	+ (not overexpressed)
9	AF647	Ki67	+	+	+	+ (T cells)
10	AF660	EpCam	+	-	+	-

The range of over expression varied widely among the 10 markers both in the cell lines and the TPs as shown in Figure3.11 below. From the Figure3.12 and table3.2 we observe that the expression level of each fluorophore from statistical analysis matches that from table. For example, CD 45 for MCF7 has negative expression and from Figure3.11 it is observed that its values is below HMI number 1 which validates it no over expression, also Daudi is positive for CD45 and from Figure3.11 it can be observed that its value is above HMI number 1 validating its over expression. Thus Xanoscope can be used to acquire data from highly multiplexed fluorophores.

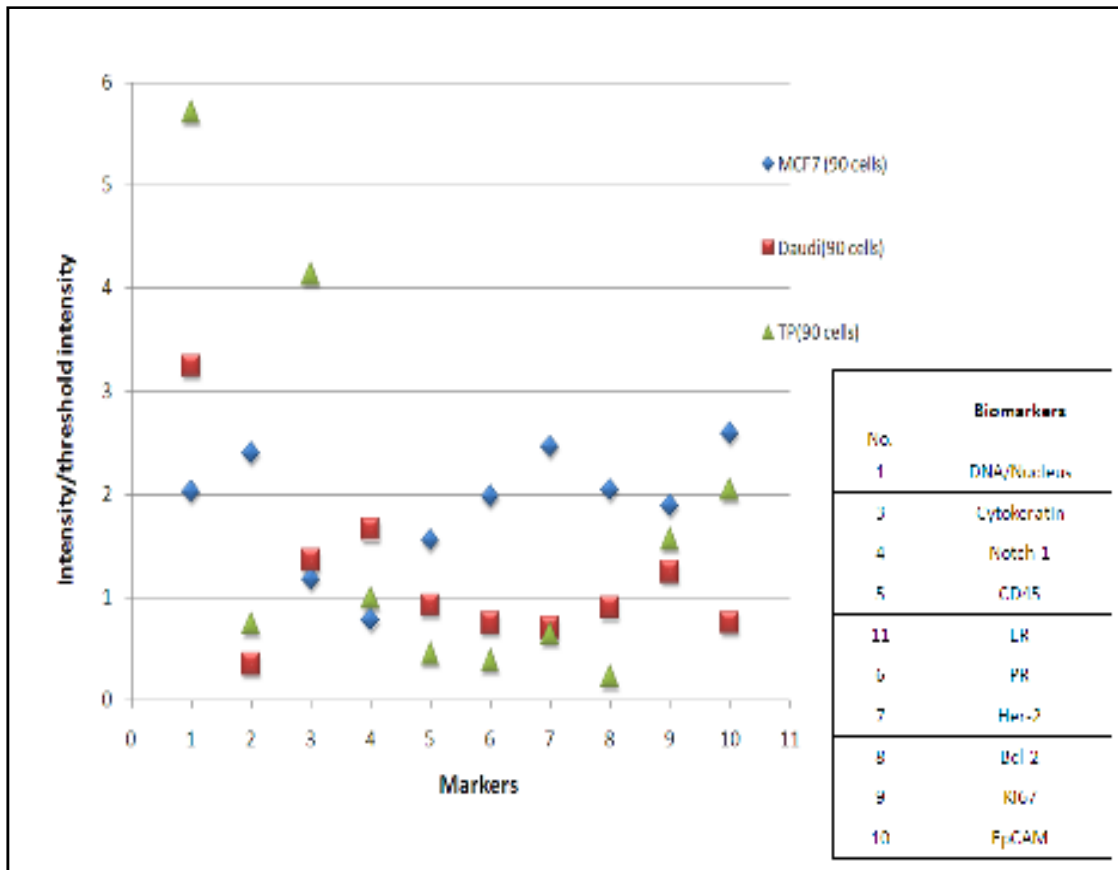


Figure 3.11 Figure shows graph of statistical analysis of the quantitative data acquired using Xanoscope. It shows normalized intensity of individual fluorophores over its threshold intensity for various cell lines and TPs. The intensity values are normalized to the threshold value of each individual fluorophore for that particular cell line or TP

CHAPTER 4

CONCLUSION AND FUTURE GOALS

Xanoscope® was developed with the goal of enabling high resolution data acquisition and control over the Hyperspectral Imaging Microscopy (HMI) system. The ability to dynamically control, the entire HMI system to provide high throughput data at minimum acquisition time is the most unique feature of Xanoscope®. The system further offers comprehensive functionality over various hardware components such as the CCD camera, imaging spectrograph and micro-mover stage that can be appropriately used depending on the applications. Once Xanoscope® was created its system parameters were validated across the specifications from individual hardware components, to prove the efficiency of the Xanoscope® system.

In order to evaluate its ability and performance, various breast cancer cell lines and TPs from breast cancer cells were multiplexed with fluorophore-antibody conjugates to identify and measure their expression levels. Standard linear unmixing technique was used to deconvolve this multiplexed fluorophores from data obtained using Xanoscope®. The measured expression levels of each fluorophore-antibody conjugate were compared against expected expression levels from literature. The results clearly indicate Xanoscope's® ability to acquire accurate data that can be used for precise quantitative simultaneous measurement of multiple tumor marker on a variety of pathology sample types. This capability of Xanoscope over HMI system has opened up new opportunities to study co-expression of multiple tumor markers within a single cell.

The future goal includes identifying more tumor marker within a single cell in a single pass. Also Xanoscope can be further developed to acquire data from unstained tissue sample and digitally assign colors to various components of a cell depending on its reference spectra. This provides means for false coloring of samples that can have a prominent impact on pathology applications. Xanoscope along with HMI system proves to be influential in diagnoses and monitoring of cancer and its response to therapeutic regimes. This thus makes Xanoscope a commercially viable system that is ready for transition into a regular pathology lab.

REFERENCES

1. Timlin, Jerilyn et al., *Hyperspectral imaging of biological targets: the difference a high resolution spectral dimension and multivariate analysis can make*. IEEE 2004, 0-7803-8388-5/04
2. Schultz, Roger et al., *Hyperspectral Imaging: A Novel Approach For Microscopic Analysis*. Cytometry 2001, 43:239–247
3. Levenson, Richard et al., *Spectral Imaging and Pathology: Seeing More*. Laboratory medicine 2004 number 4: volume 35
4. Levenson, Richard et al., *Spectral Imaging and microscopy*. American laboratory November 2000
5. Huebschman, Michael et al., *Hyperspectral Imaging*. Elsevier 2004 OPTC00704
6. Huebschman, Michael et al., *Characteristics and Capabilities of Hyperspectral Imaging Microscope*. IEE2002 0739-5175/02.
7. Bautista, Pinky et al., *Digital Staining of Unstained Pathological Tissue Samples through Spectral Transmittance Classification*. OPTICAL REVIEW 2005 Vol. 12, No. 1
8. Keshava, Nirmal et al. *Spectral unmixing* IEEE 2002 1053-5888/02
9. Shah, Bhavesh, *Characterization of a noninvasive, in vivo, microscopic Hyperspectral imaging system for microvascular visualization*. 2006 UMI Number: 1433784
10. Weissleder, Ralph et al., *Imaging in the era of molecular oncology*. Nature 2008 doi:10.1038
11. Haraguchi, Tokuko et al., *Spectral imaging fluorescence microscopy*. Genes to Cells 2002 881–887

12. Sinclair, Michael et al., *Design, construction, characterization, and application of a hyperspectral microarray scanner*. Optical Society of America 2004 0003-6935_04_102079-10
13. Kumar, Sonia et al., *Optical molecular imaging agents for cancer diagnostics and therapeutics*. *Medicine*, 2006
14. Fong, Alexandre et al., *Hyperspectral Imaging for the Life Sciences*. Biophotonics International 2008
15. Siddiqi, Anwer et al., *Use of Hyperspectral Imaging to Distinguish Normal, Precancerous, and Cancerous Cells*. American Cancer Society 2008 DOI 10.1002/cncr.23286
16. Papadakis, Antonis et al. *A Novel Spectral Microscope System: Application in Quantitative Pathology*. IEEE2003 0018-9294
17. True, Lawrence et al., *Quantum Dots for Molecular Pathology*. Journal of Molecular Diagnostics 2007 Vol. 9, No. 1
18. Kopolovic, Barshack et al., *Spectral morphometric characterization of breast carcinoma cells*. British Journal of Cancer 1999 79(9/10), 1613–1619
19. Zimmermann, Timo et al., *Spectral imaging and its applications in live cell microscopy*. Elsevier 2003 0014-5793
20. Imaging Spectrograph: Operating Instructions Manual from Acton Research Corporation SpectraPro-500i
21. Stage Motor: MAC 2000 Configuration Manual
22. Charge Couple Device (CCD) : Quantix 1602E Data sheet
23. Fluorophores and its application in hyperspectral imaging:
<http://www.olympusfluoview.com/theory/fluorophoresintro.html>
24. Epi-Fluorescence Microscope System:
<http://www.olympusmicro.com/primer/techniques/fluorescence/ix70fluorescence.html>
25. Typical Dispersion Grating in Imaging Spectrograph :
<http://www.princetoninstruments.com/Uploads/Princeton/Documents/Datasheets>

26. Analogy for Charge transfer in a Typical CCD Camera:
<http://www.microscopyu.com/articles/digitalimaging/ccdintro.html>
27. Binning: <http://www.microscopyu.com/articles/digitalimaging/ccdintro.html>
28. RS232 Character Frame: <http://francis.courtois.free.fr/jc1/serial/Basics/BitFormat.html>
29. Fluorophores: <http://probes.invitrogen.com/handbook/sections/0001.html>
30. Multispectral Imaging: <http://www.ecse.rpi.edu/~roysam/CTIA/Lecture-slides-2008/>
31. Light Microscopy: www.zmb.unizh.ch.
32. www.csiro.org

BIOGRAPHICAL INFORMATION

Dipen Rana was born in the economic capitol of India, Mumbai, and has to his credit Bachelor of Instrumentation Engineering degree at Mumbai University conferred in August 2005. He joined University of Texas at Arlington in the Fall 2006 semester, to pursue Masters Degree in Biomedical Engineering. Current research focus pertains to the work in the field of Software and Hardware solutions for Medical Imaging, especially Hyperspectral Imaging.